



HAL
open science

Discrete kinetic theory for 2D modelling of a moving crowd: Application to the evacuation of a non-connected bounded domain.

Abdelghani Elmoussaoui, Pierre Argoul, M El Rhadi, A Hakim

► **To cite this version:**

Abdelghani Elmoussaoui, Pierre Argoul, M El Rhadi, A Hakim. Discrete kinetic theory for 2D modelling of a moving crowd: Application to the evacuation of a non-connected bounded domain.. Computers & Mathematics with Applications, 2017, 31 p. 10.1016/j.camwa.2017.10.023 . hal-01684645

HAL Id: hal-01684645

<https://hal.science/hal-01684645>

Submitted on 15 Jan 2018

HAL is a multi-disciplinary open access archive for the deposit and dissemination of scientific research documents, whether they are published or not. The documents may come from teaching and research institutions in France or abroad, or from public or private research centers.

L'archive ouverte pluridisciplinaire **HAL**, est destinée au dépôt et à la diffusion de documents scientifiques de niveau recherche, publiés ou non, émanant des établissements d'enseignement et de recherche français ou étrangers, des laboratoires publics ou privés.

Discrete kinetic theory for 2D modelling of a moving crowd : Application to the evacuation of a non-connected bounded domain.

A. Elmoussaoui^a, P. Argoul^{b,c}, M. El Rhabi^{a,d}, A. Hakim^a

^aLAMAI, FST Marrakech, Université Cadi Ayyad, Morocco

^bUniversité Paris-Est, LVMT (UMR-T 9403), Ecole des Ponts ParisTech,
IFSTTAR, UPEMLV, F-77455 Marne la Vallée, France

^cUniversité Paris-Est, MAST, SDOA, IFSTTAR, F-77447 Marne-la-Vallée, France

^dIMI, Ecole des Ponts ParisTech, Université Paris Est, France

Abstract

This paper concerns the mathematical modelling of the motion of a crowd in a non connected bounded domain, based on kinetic and stochastic game theories. The proposed model is a mesoscopic probabilistic approach that retains features obtained from both micro- and macro- scale representations; pedestrian interactions with various obstacles being managed from a probabilistic perspective. A proof of the existence and uniqueness of the proposed mathematical model's solution is given for large times. A numerical resolution scheme based on the splitting method is implemented and then applied to crowd evacuation in a non connected bounded domain with one rectangular obstacle. The evacuation time of the room is then calculated by our technique, according to the dimensions and position of a square-shaped obstacle, and finally compared to the time obtained by a deterministic approach by means of randomly varying some of its parameters.

Keywords: Discrete kinetic theory, Complex system, Evacuation, Crowd dynamics, Splitting scheme

1. Introduction

The dynamic modelling of crowd motion has recently aroused a great interest in the scientific community and is used in numerous applications, such as engineering and social science [1]. It has become increasingly important to avoid or control panic situations and to ensure the safety of people in congested areas.

5 Mathematical representations of crowd motion from the microscopic to macroscopic scale have been an active field of study for the last two decades, with a rich scientific literature [2, 3, 4, 5, 6]. The aim of this paper is not to present an exhaustive list of references. Only some of the most frequently used will be mentioned: the microscopic approach based on the social forces model, proposed by Helbing [4, 5], where the movement of the crowd is characterized by the position and velocity of each individual, and the macroscopic models, given by Hughes [6], that
10 consider the crowd as a fluid.

*Corresponding author: A. Hakim

Email addresses: elmoussaoui.abdelghani@gmail.fr (A. Elmoussaoui), mohammed.el-rhabi@enpc.fr (M. El Rhabi), pierre.argoul@ifsttar.fr (A. Hakim), abdelilah.hakim@gmail.com (A. Hakim)

Recently, an intermediate mesoscopic representation based on the kinetic approach appeared and its application to crowd representation gave promising results for the description of pedestrians' strategy. Very few references of the mesoscopic representation can be found in the literature [7, 8, 9, 10, 11].

15

The kinetic theory is a mathematical description of a volume of material containing a large number of particles interacting with each other, for example, a volume of gas particles [12]. This approach allows us to connect both the macroscopic and microscopic properties. Monte Carlo particle methods have a relevant role in the numerical resolution of kinetic equations [13, 14]. Moreover, this theory has been applied in many areas, namely, modelling of vehicular traffic [15, 16], and crowd dynamics [7, 8, 9, 10, 11, 17, 18], which is the subject of this study.

The modelling of a crowd by a kinetic approach started with Bellomo's and Bellouquid's work [9], in which the set of main governing equations are introduced. In this approach, the crowd is seen as a complex system in which the interactions between people (particles) are managed from a probabilistic point of view and the microscopic state of each pedestrian (particle) is characterized by his/her position and speed. In addition, the general form of the system is represented by a distribution function in a microscopic state and the dynamic of this distribution function is given by the study of particles balance in a unit volume element of the phase plane. Then Bellomo et al. [8] developed this approach and handled the movement of a crowd moving in different directions, in an unbounded domain and where the objective of each particle is to reach a fixed target. Afterwards, Agnelli et al. [7] studied the case of people moving in a connected bounded domain, without obstacles. Then Bellomo and Gibelli treated the density-velocity diagram in steady flow conditions and studied some collective emerging behaviors that are experimentally observed, namely the self-organized behaviors leading to the creation of lanes in streets and the increasing of evacuation time in stressful conditions [17].

Most of the studies that were previously mentioned, concerned connected areas [7, 8, 9, 17], while the question of non connected areas is still open. In this paper, the kinetic theory applied to crowd dynamics is extended to its motion in a non-connected bounded domain, with the presence of fixed obstacles. To model interactions, it is assumed that pedestrians can change their direction for various reasons, such as: the wish to reach a target, the avoidance of the edges of the domain and / or fixed obstacles in the field. In a future step, pedestrians will be considered as "active particles" by taking into account their heterogeneity and their capacity to develop a strategy of displacement.

This paper is organized as follows: Section 2 provides the mathematical model for the crowd evacuation in an area including walls and obstacles. Then, probabilistic tools are used to describe pedestrian-pedestrian interactions as well as pedestrians interactions along with the geometry of the area. Section 3 presents a mathematical framework to obtain proofs of the existence and of the uniqueness of the proposed model's solution. Section 4 is devoted to numerical simulations to check the ability of the proposed model to describe the main features of the pedestrian dynamics, particularly the avoidance of fixed obstacles on their walk towards the exit. The influence of the position of a fixed square obstacle in the vicinity of the exit is finally studied with respect to the evacuation time for a group of 50 persons.

2. Position of the problem under study. Mathematical modelling

Let us consider a system composed of N particles (the pedestrians) distributed randomly in a two-dimensional bounded domain $\Omega \subset \mathbb{R}^2$.

This group of N pedestrians present in the room at initial time t_0 , wish to evacuate the room by the exit of size S . At initial time $t = t_0$, pedestrians are distributed within a disk \mathcal{D}_0 of radius r and of center $M_0(x_0, y_0)$. The initial global density is then: $\rho_0 = \frac{N}{\pi r^2} (\text{ped}/m^2)$.

Kinetic type equations derivation requires a detailed analysis of the interactions at a micro-scale, namely at the pedestrian scale related to the statistical representation of the overall system; this requires a suitable probability distribution over the micro-state.

This particle distribution function is given by: $f = f(t, \mathbf{x}, \mathbf{v})$ for all $t \geq t_0$, $\mathbf{x} \in \Omega$, $\mathbf{v} \in D_{\mathbf{v}}$, where $D_{\mathbf{v}}$ represents the domain of velocities.

If $f(t, \mathbf{x}, \mathbf{v})$ is locally integrable in \mathbf{x} , then $f(t, \mathbf{x}, \mathbf{v})d\mathbf{x}d\mathbf{v}$ represents the number of individuals, located at time t in an infinitesimal rectangle $[x, x + dx] \times [y, y + dy]$ with the velocity belonging to $[v_x, v_x + dv_x] \times [v_y, v_y + dv_y]$, where: $\mathbf{x} = (x, y)$ and $\mathbf{v} = (v_x, v_y)$.

If $f(t, \mathbf{x}, \mathbf{v})$ is locally integrable in \mathbf{v} , the local density (the number of people per square meter) at the point \mathbf{x} and time t can be introduced:

$$\rho(t, \mathbf{x}) = \int_{D_{\mathbf{v}}} f(t, \mathbf{x}, \mathbf{v})d\mathbf{v}. \quad (1)$$

At initial time t_0 , it can be written that: $\rho(t_0, \mathbf{x}) = \rho_0 \mathbf{1}_{\mathcal{D}_0}(\mathbf{x})$ where $\mathbf{1}_{\mathcal{D}_0}(\mathbf{x})$ is the indicator function of the subset \mathcal{D}_0 .

The impact of crowd density for a standing crowd and a moving crowd is important to understand for crowd safety. In the UK Guides produced to advise on crowd safety issues (cf. [19]), the safety limit for crowd density is stated as 4 pedestrians per square meter for a moving crowd and 4.7 for standing areas. To be closer to reality, the individual dimensions of pedestrians must be taken into account in the density analysis. For a totally packed metro train (French RATP), the density is between 6 and 8 pedestrians $/m^2$. In conclusion, a maximum value ρ_{max} for local crowd density, $\rho_{max} \leq 8$ pedestrians $/m^2$, is introduced, and a maximum number of pedestrians N_{max} is then deduced: $N_{max} = \pi r^2 \rho_{max}$.

In our model, dimensionless quantities are preferred. To do that, from the following reference variables:

- L : a characteristic length of the domain Ω , for example its diagonal when Ω is rectangle shaped,
- V_m : the maximum speed of the pedestrian walking unobstructed in the environment,
- T_m : a reference value for the evacuation time is given by: $T = L/V_m$,
- ρ_{max} : the maximum local crowd density,

the following unit-less variables are then defined:

- the position variable: $\tilde{\mathbf{x}} = \frac{\mathbf{x}}{L}$.
- the time: $\tilde{t} = \frac{t}{T}$.

- the velocity modulus: $\tilde{v} = \frac{v}{\tilde{v}_m}$,

- The distribution function: $\tilde{f} = \frac{f}{\rho_{max}}$, leading to $\tilde{\rho} = \frac{\rho}{\rho_{max}}$.

In the following, for the sake of simplicity, the tildes are omitted.

2.1. Representation of the pedestrian environment

The bounded domain $\Omega \subset \mathbb{R}^2$, in which pedestrians move, is a room of rectangular shape of length L_x and width L_y . Its external border is made of walls and is noted W .

- A single obstacle noted by Or with ∂Or being its boundary is added within Ω . In the following, the obstacle is rectangle-shaped with sides of length L_{obs} and width l_{obs} . A reference frame $(O, \mathbf{e}_x, \mathbf{e}_y)$ is defined and polar coordinates are preferred. For the sake of simplicity, this study is limited to the case of a single obstacle cf. Fig.1, but the geometry of the domain can be further modified by inserting several obstacles of different shapes.

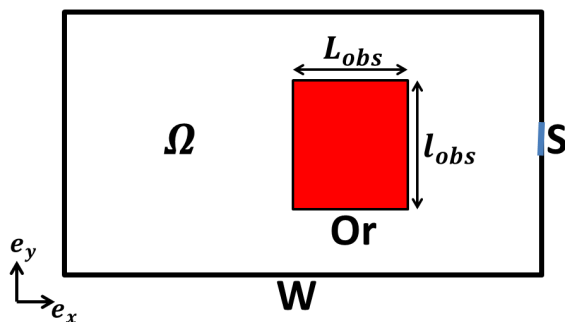


Figure 1: Illustration of the walking domain. W : wall, Or : rectangular obstacle, S : exit, $\partial\Omega = W \cup S \cup \partial Or$ (with ∂Or is the obstacle's border).

Two parameters already present in [17] are finally introduced $\alpha \in [0, 1]$ and $\xi \in [0, 1]$, respectively.

- α is related to the quality of the domain : when $\alpha = 0$, the domain is of poor quality, that means that pedestrians are forced to stop walking, while when $\alpha = 1$, the quality of the domain is maximum, allowing a pedestrian to walk with the highest speed. ξ characterizes the strength of the pedestrian's preference for areas of low pedestrian density and it is supposed to give indication of the level of pedestrians' anxiety.

2.2. modelling the velocity vector

The approach developed in the present work refers to the hybrid approach reviewed in [7, 8], where the discrete variable for the individual velocity states θ , defined by the angle of the selected velocity \mathbf{v} direction with \mathbf{e}_x , is used. The velocity vector can then be expressed as

$$\mathbf{v}[\rho] = v[\rho](t, \mathbf{x}) \cos(\theta) \mathbf{e}_x + v[\rho](t, \mathbf{x}) \sin(\theta) \mathbf{e}_y,$$

where $v[\rho]$ is the speed; square brackets are used to denote that \mathbf{v} can depend on ρ in a functional way, for instance on ρ and on its gradient $\frac{\partial \rho}{\partial \mathbf{x}}$.

The speed variation depends on the interactions between pedestrians. Specifically, pedestrians adjust their velocity modulus according to the level of congestion around them and on the environmental conditions. In this paper, the dependence of the velocity on the local density is motivated by the fundamental diagram developed in [17]. The main idea is that the velocity of the pedestrian decreases monotonically with the density from the maximal value $v[\rho = 0] = 1$ of $\rho = 0$ to $v[\rho = 1] = 0$ where $\rho = 1$, corresponding to the maximal density. Moreover, the maximal velocity observed at very low density increases with the quality of the environmental conditions and / or the pedestrian's anxiety.

From the density speed diagram developed in [17], the following density speed is deduced:

$$v[\rho](t, \mathbf{x}) = \frac{\sigma^3 (1 - \rho(t, \mathbf{x}))^2}{\sigma^2 (1 - \rho(t, \mathbf{x}))^2 + (1 - \sigma) \rho^2(t, \mathbf{x})}, \quad (2)$$

95 where $\sigma = \alpha \xi$; the parameters α and ξ , previously introduced, characterize respectively the quality of the domain, and the trend of pedestrians to adapt their walk to their surroundings instead of searching for less crowded areas.

2.3. Mathematical model equations

The number of pedestrians N is limited by the maximum number N_{max} and generally not large enough to justify the continuity assumption of the particle distribution function with respect to the velocity. Indeed, it is assumed that the velocity directions θ_i take discrete values in the following set:

$$S_\theta = \left\{ \theta_i = \frac{i-1}{n} 2\pi : i = 1, \dots, n \right\}.$$

Therefore, due to the deterministic nature of the variable v , the distribution function can be expressed as :

$$f(t, \mathbf{x}, \theta) = \sum_{i=1}^n f_i(t, \mathbf{x}) \delta(\theta - \theta_i), \quad (3)$$

where δ is the Dirac distribution; $f_i(t, \mathbf{x}) = f(t, \mathbf{x}, \theta_i)$, represents pedestrians, viewed as active particles, moving in direction θ_i , at time t and position \mathbf{x} , per unit area.

The local density $\rho(t, \mathbf{x})$ previously defined in Eq. (1), becomes the sum of $f_i(t, \mathbf{x})$ for $1 \leq i \leq n$:

$$\rho(t, \mathbf{x}) = \sum_{i=1}^n f_i(t, \mathbf{x}). \quad (4)$$

The derivation of the mathematical structure used in the present paper refers to the theory developed in [8], where the mathematical model is obtained by a balance of particles in a unit volume of the micro state space. Indeed, the motion of a particles group (pedestrians) is governed by the partial derivative equation (PDE) of transport applied to f_i with a second member Γ_i characterizing the different interactions between pedestrians with their environment:

$$\partial_t f_i(t, \mathbf{x}) + \mathbf{v}_i[\rho](t, \mathbf{x}) \cdot \partial_{\mathbf{x}} f_i(t, \mathbf{x}) = \Gamma_i(t, \mathbf{x}) \quad i = 1, \dots, n, \quad (5)$$

where: $\mathbf{v}_i[\rho](t, \mathbf{x}) = v[\rho](t, \mathbf{x}) (\cos(\theta_i), \sin(\theta_i))^T$ and $\partial_{\mathbf{x}} = (\partial_x, \partial_y)^T$. This $\Gamma_i(t, \mathbf{x})$ term also allows us to take into account boundary conditions (walls W and the obstacle's borders ∂Or).

100 *2.4. Modelling of interactions*

By referring to [7, 11, 17], modelling the interactions is a decision process in which each particle moves along with the others as well as within the geometry of the domain. The interaction involves three types of particles:

- The test particle with micro-state (\mathbf{x}, θ_i) and distribution function $f_i(t, \mathbf{x}) = f(t, \mathbf{x}, \theta_i)$.
- The field particle with micro-state (\mathbf{x}^*, θ_k) and distribution function $f_k(t, \mathbf{x}) = f(t, \mathbf{x}^*, \theta_k)$.
- 105 • The candidate particle with micro-state (\mathbf{x}, θ_h) and distribution function $f_h(t, \mathbf{x}) = f(t, \mathbf{x}, \theta_h)$.

The candidate particle can acquire, in probability, the micro-state of the test particle after interaction with the field particles, while the test particle loses its state in the interaction with the field particles.

Two types of interactions are considered, those between candidate and field particles and those between candidate particle and obstacle (either within the domain or the border walls themselves).

In this way the right hand side of eq.(5) can be decomposed in two terms as: $\Gamma_i = \Gamma_i^P + \Gamma_i^D$, where Γ_i^P refers to interactions between pedestrians and Γ_i^D to interactions between pedestrians and obstacles (either present within the domain or against the border walls). Both terms are detailed in the following sub-paragraphs.

115 *2.4.1. The Γ_i^P term*

The term Γ_i^P of interactions between pedestrians (particles) is defined in a probabilistic sense, since pedestrians will not react in the same way when facing a particular situation. Interactions of test and candidate particle with field particle can be modeled by the following quantities:

- Interaction domain (visibility zone) : it represents the area where the trajectory of each candidate pedestrian can be influenced by those of other field pedestrians, which can be defined as circular sector with radius V symmetric with respect to the velocity direction defined by the visibility angle ϕ (see fig.2):

$$V(\mathbf{x}, \mathbf{e}_d, R_V, \phi) = \left\{ \mathbf{y} \in \Omega / \|\mathbf{x} - \mathbf{y}\|_2 \leq R_V, \frac{\mathbf{y} - \mathbf{x}}{\|\mathbf{y} - \mathbf{x}\|_2} \cdot \mathbf{e}_d \geq \cos(\phi) \right\}.$$

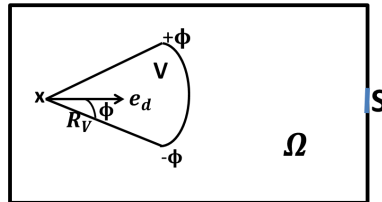


Figure 2: Vision field V for a pedestrian located at the point \mathbf{x} with unit velocity direction \mathbf{e}_d .

120

This visibility zone is introduced just when a pedestrian located at the point \mathbf{x} , interacts with the other pedestrians, but it not introduced in the case of interaction with obstacles and walls.

- The interaction rate $\eta[\rho(t, \mathbf{x})]$ characterizes the contact frequency that a candidate h-pedestrian (or test) in \mathbf{x} develops with a field k-pedestrian in the visibility zone V . The use of the same idea developed in [7] is proposed, by treating the interaction rate with increasing local density $\eta[\rho(t, \mathbf{x})] = \eta_0 \rho(t, \mathbf{x})$, where η_0 is a constant.

125

- The transition probability density $B_{hk}(i)$, characterizes the fact that the candidate pedestrian changes his/her direction θ_h to the test pedestrian's direction θ_i , due to the interaction with field pedestrians of a direction θ_k . This probability is assumed to be dependent on the density of pedestrians $\rho(t, \mathbf{x})$.

The probabilities $B_{hk}(i)$ of each i-th pedestrian satisfy the following relationship:

$$\sum_{i=1}^n B_{hk}[\rho(\mathbf{x})](i) = 1 \quad \text{for } k, h = 1, \dots, n. \quad (6)$$

The probability transition definition depends on the desired direction more precisely on the preferred angle of motion θ_d^p , that will be defined in the next paragraph.

It is referred to [10, 17] for the definition of the preferred angle of motion. Indeed, due to the assumption of the deterministic nature of the speed v , interactions between particles are assumed to modify their dynamics by changing the direction of motion. The assumed walking direction modified by two types of stimuli: (1) the tendency to follow the stream and (2) the attempt to avoid overcrowded areas. These are represented by two unit vectors $\mathbf{e}^{(v)}$, $\mathbf{e}^{(s)}$, respectively. It is expected that at high density pedestrians move in the direction $\mathbf{e}^{(v)}$. Conversely at low density they tend to follow the stream in the direction $\mathbf{e}^{(s)}$. Indeed, the desired direction is defined as follows:

$$\mathbf{e}_d^p = \frac{\sigma \mathbf{e}^{(v)} + (1 - \sigma) \mathbf{e}^{(s)}}{\|\sigma \mathbf{e}^{(v)} + (1 - \sigma) \mathbf{e}^{(s)}\|_2}, \quad (7)$$

where,

- $\mathbf{e}^{(v)} = (\cos(\theta_m), \sin(\theta_m))$ with $m = \arg \min_{j=1, \dots, n} \partial_j \rho$, ∂_j is the derivative of ρ in the direction θ_j .
- $\mathbf{e}^{(s)} = (\cos(\theta_k), \sin(\theta_k))$ defines the direction of the particle.
- The preferred angle θ_d^p which allows pedestrians to follow the stream and to avoid overcrowded areas obtained from (7), through the relation: $\mathbf{e}_d^p = (\cos(\theta_d^p), \sin(\theta_d^p))^T$.

130

It is assumed that each pedestrian can rest in her/his initial state or change his/her direction, in the clockwise direction or in the opposite clockwise direction in the set S_ρ . This means that a pedestrian is located either in the states, $h + 1$, $h - 1$ or remains in state h . Three cases defined and illustrated in Table 1 are considered according to the position of θ_d^p from θ_h .

135

<i>Case 1</i> : $\theta_d^p < \theta_h$	$B_{hk}[\rho](i) = \begin{cases} \sigma \rho & \text{if } i = h - 1 \\ 1 - \sigma \rho & \text{if } i = h \end{cases}$
<i>Case 2</i> : $\theta_h < \theta_d^p$	$B_{hk}[\rho](i) = \begin{cases} 1 - \sigma \rho & \text{if } i = h \\ \sigma \rho & \text{if } i = h + 1 \end{cases}$
<i>Case 3</i> : $\theta_h = \theta_d^p$	$B_{hk}[\rho](i) = \begin{cases} 1 & \text{if } i = h \\ 0 & \text{else} \end{cases}$

Table 1: Definition and illustration of the probability term $B_{hk}[\rho](i)$.

The interaction term between pedestrians Γ_i^P is defined as the difference between the gain and the loss of pedestrians moving in the direction θ_i due to the interactions with other pedestrians:

$$\Gamma_i^P(t, \mathbf{x}) = \sum_{h=1}^n \sum_{k=1}^n \int_V \eta[\rho(t, \mathbf{x}^*)] B_{hk}(i) [\rho(t, \mathbf{x}^*)] f_h(t, \mathbf{x}) f_k(t, \mathbf{x}^*) d\mathbf{x}^* - f_i(t, \mathbf{x}) \sum_{h=1}^n \int_V \eta[\rho(t, \mathbf{x}^*)] f_h(t, \mathbf{x}^*) d\mathbf{x}^*. \quad (8)$$

2.4.2. The Γ_i^D term

This term is introduced to account for boundary conditions, more precisely to model interactions with walls and obstacles. In this sense, we refer to [7]. The assumptions used in the following are summarized below:

- A pedestrian can change his/her direction, due to
 1. his/her willingness to reach the exit.
 2. the presence of walls or fixed obstacles in front of him/her.

The Γ_i^D term characterizes the interactions between pedestrians and obstacles within the walking area during the evacuation phase. In a similar way as for the Γ_i^P term, the Γ_i^D is modeled by means of the following two interaction terms:

- $P_h(i)$ the probability of the event that the pedestrian changes its direction θ_h into the direction θ_i , due to the presence of walls W , to the obstacle Or and to the exit S , is then introduced. This probability satisfies the following relation:

$$\sum_{i=1}^n P_h(i) = 1 \quad \text{for } h = 1, \dots, n, \quad (9)$$

and its definition depends on the desired direction $\mathbf{e}_d(\mathbf{x})$ for each pedestrian at position \mathbf{x} , and more precisely on the angle θ_d that $\mathbf{e}_d(\mathbf{x})$ makes with $\mathbf{e}_\mathbf{x}$.

In the same way, three cases defined and illustrated in Table 2 are considered according to the position of θ_d from θ_h .

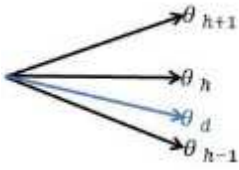
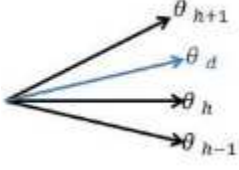
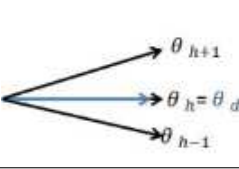
Case 1 : $\theta_d < \theta_h$	$P_h(i) = \begin{cases} \alpha & \text{if } i = h-1 \\ 1-\alpha & \text{if } i = h \end{cases}$	
Case 2 : $\theta_h < \theta_d$	$P_h(i) = \begin{cases} 1-\alpha & \text{if } i = h \\ \alpha & \text{if } i = h+1 \end{cases}$	
Case 3 : $\theta_h = \theta_d$	$P_h(i) = \begin{cases} 1 & \text{if } i = h \\ 0 & \text{else} \end{cases}$	

Table 2: Definition and illustration of probability's term $P_h(i)$, where $\alpha \in [0, 1]$ sets the quality of the domain.

- $\mu[\rho(t, \mathbf{x})]$ is an interaction rate, $0 < \mu[\rho(t, \mathbf{x})] \leq 1$, that characterizes the frequency of interactions between the pedestrians and the field. It is a decreasing function of the local density.

The interaction term Γ_i^D between pedestrians and the area characterizes the difference between the gain and the loss of the particles moving in the direction θ_i and is given by:

$$\Gamma_i^D(t, \mathbf{x}) = \mu[\rho(t, \mathbf{x})] \left(\sum_{h=1}^n P_h(i) f_h(t, \mathbf{x}) - f_i(t, \mathbf{x}) \right). \quad (10)$$

155 2.4.3. Determination of the desired direction unit vector \mathbf{e}_d

It is then proposed to represent the desired direction unit vector \mathbf{e}_d for each pedestrian by a sum of three vectors: the $\boldsymbol{\gamma}(\mathbf{x})$ vector models the direction which allows the pedestrian to avoid the obstacle, the $\boldsymbol{\tau}(\mathbf{x})$ vector models the pedestrian direction to avoid the walls and finally $\boldsymbol{\nu}(\mathbf{x})$ models the direction which allows the pedestrian to go toward the exit:

$$\mathbf{e}_d(\mathbf{x}) = \frac{\boldsymbol{\gamma}(\mathbf{x}) + \boldsymbol{\tau}(\mathbf{x}) + \boldsymbol{\nu}(\mathbf{x})}{\|\boldsymbol{\gamma}(\mathbf{x}) + \boldsymbol{\tau}(\mathbf{x}) + \boldsymbol{\nu}(\mathbf{x})\|_2}. \quad (11)$$

The directions contribute to the desired direction defined by the previous linear combination defined in eq.(11). This assumption is a simplification of reality.

To define these three vectors, the domain Ω is decomposed into three zones: the obstacle's influence zone Z ,
 160 the security zone Z_s to ensure the non collision between pedestrians and the walls, and finally a neutral zone Z_n where pedestrians have only the wish to go toward the exit. These three zones are illustrated in Fig.3.

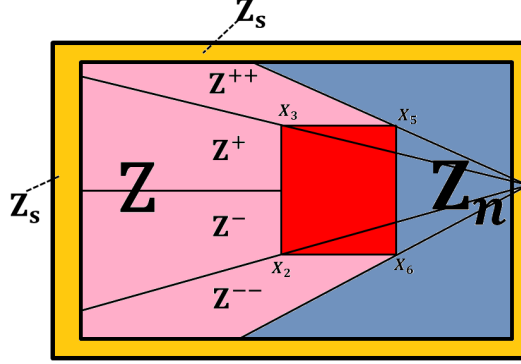


Figure 3: Representation of the three zones: $Z = Z^+ \cup Z^- \cup Z^{++} \cup Z^{--}$, the obstacle's influence zone for pedestrians, Z_n the neutral zone, and Z_s the security zone.

The vector field $\gamma(\mathbf{x})$ which models the direction that allows pedestrians to avoid the obstacle, is defined by:

$$\gamma(\mathbf{x}) = \begin{cases} \beta_1(\mathbf{x}) + \beta_2(\mathbf{x}) & \mathbf{x} \in Z^-, \\ \beta_3(\mathbf{x}) + \beta_4(\mathbf{x}) & \mathbf{x} \in Z^+, \\ \mathbf{e}_x & \mathbf{x} \in Z^{++} \cup Z^{--}, \\ 0 & \mathbf{x} \in Z_n \cup Z_s, \end{cases} \quad (12)$$

where:

$$\beta_i(\mathbf{x}) = \frac{\mathbf{x}_i - \mathbf{x}}{\|\mathbf{x}_i - \mathbf{x}\|_2} \quad i = 1, 2, 3, 4.$$

- $\mathbf{x}_2, \mathbf{x}_3$ are two vertices of the obstacle on the opposite side to the exit.
- $\mathbf{x}_1, \mathbf{x}_4$ are respectively the intersection points between the straight line $(\mathbf{x}_2\mathbf{x}_3)$ and two straight lines Δ_1, Δ_2 defining the influence area Z , (see fig. 4).

$\nu(\mathbf{x})$ is the vector field, which models the direction that allows pedestrians to go toward the exit (see fig.5), and is given by the following expression:

$$\nu(\mathbf{x}) = \begin{cases} \mathbf{b}_1(\mathbf{x}) + \mathbf{b}_2(\mathbf{x}) & \text{if } \mathbf{x} \in Z_n, \\ 0 & \text{else,} \end{cases} \quad (13)$$

where:

$$\mathbf{b}_i(\mathbf{x}) = \frac{\mathbf{x}_{s_i} - \mathbf{x}}{\|\mathbf{x}_{s_i} - \mathbf{x}\|_2} \quad i = 1, 2,$$

¹⁶⁵ $\mathbf{x}_{s1}, \mathbf{x}_{s2}$ are coordinates of the nodes that define the exit.

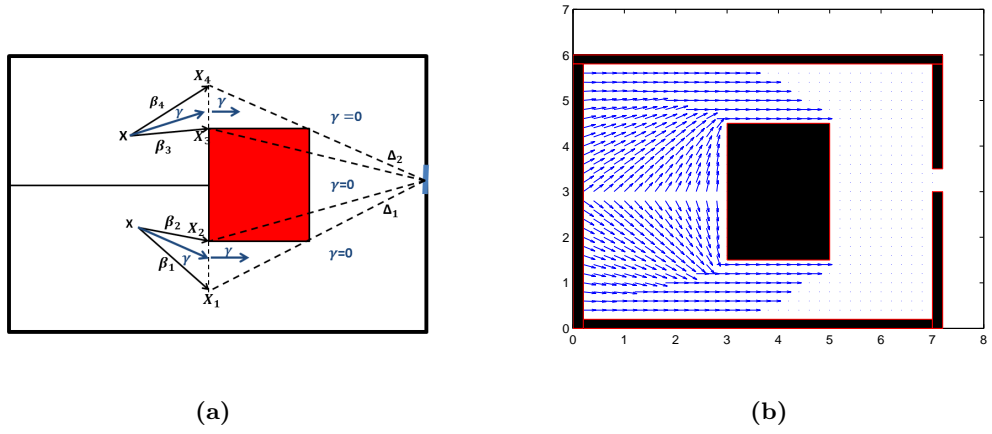


Figure 4: (a) Illustration of the construction of the $\gamma(\mathbf{x})$ vector which models the direction allowing each pedestrian to avoid the obstacle Or , and (b) the γ vector at any point \mathbf{x} of the domain Ω .

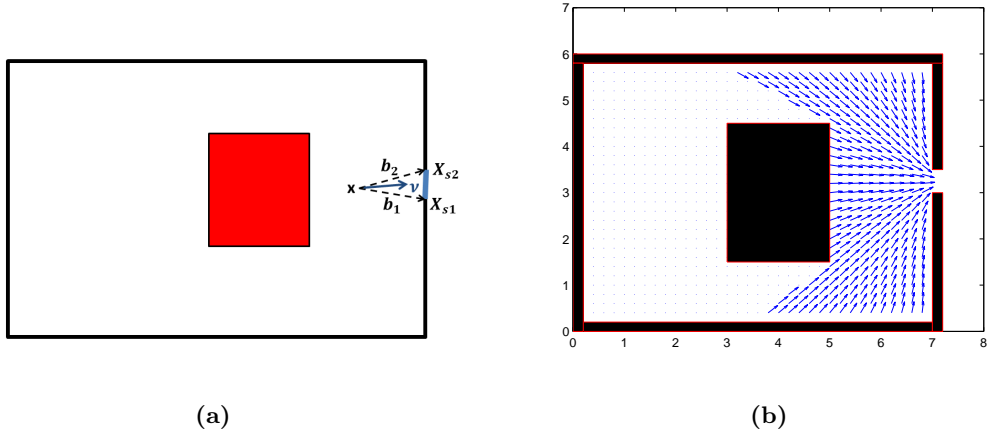


Figure 5: (a) Illustration of the construction of the $\nu(\mathbf{x})$ vector which models the direction allowing the pedestrian to go to the exit, and (b) the ν vector in any point \mathbf{x} of the domain Ω .

Finally the field vector $\tau(\mathbf{x})$ which models the direction to avoid collisions between individual pedestrians and the walls is defined as follows:

$$\tau(\mathbf{x}) = \begin{cases} \mathbf{e}_x & \mathbf{x} \in Z_{S1}, \\ -\mathbf{e}_y & \mathbf{x} \in Z_{S2}, \\ \mathbf{e}_y & \mathbf{x} \in Z_{S3}, \\ 0 & \text{else,} \end{cases} \quad (14)$$

where the security zone is divided in 3 areas: Z_{S1} , Z_{S2} and Z_{S3} (see fig.6).

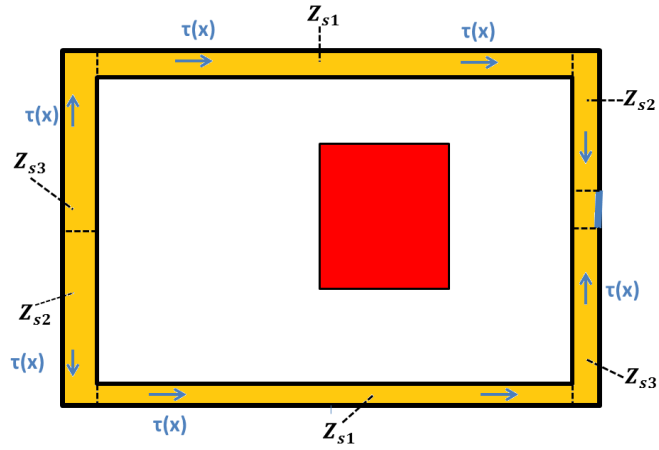


Figure 6: Illustration of $\tau(\mathbf{x})$ vector which models the direction allowing the pedestrian to avoid the walls.

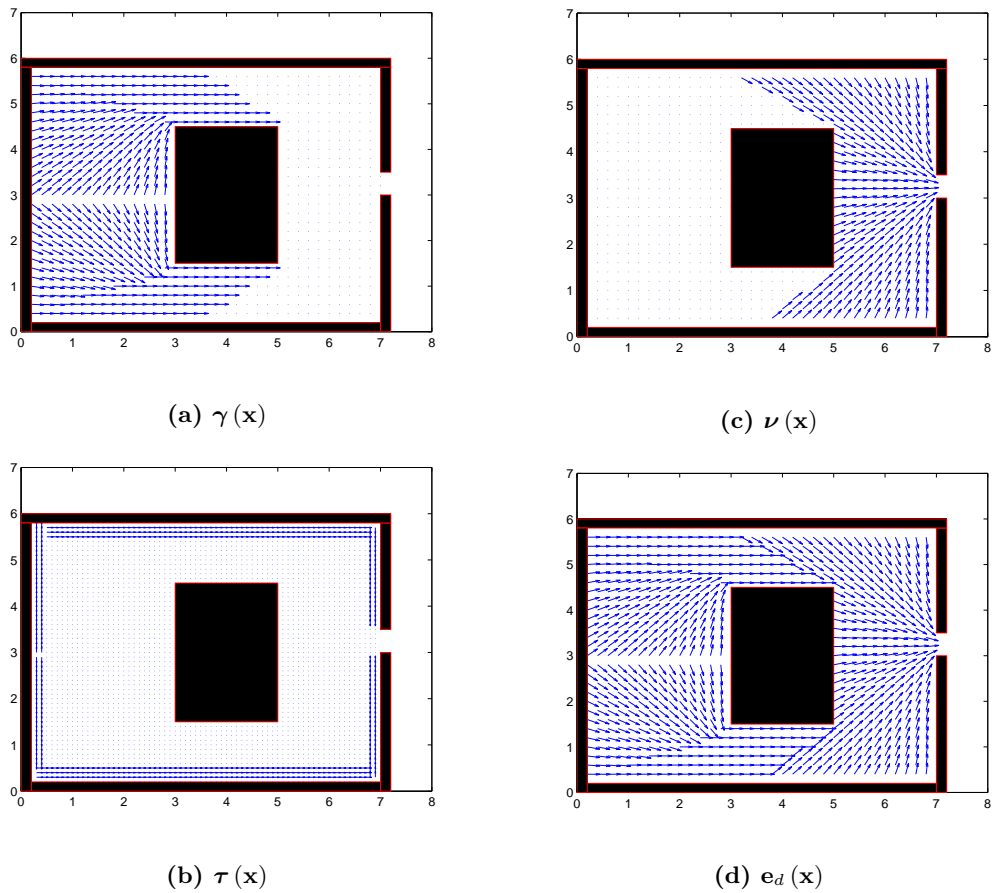


Figure 7: Illustration of vectors modelling the direction allowing pedestrians to avoid walls, the obstacle and to go toward the exit, (a): $\gamma(\mathbf{x})$, (b): $\tau(\mathbf{x})$, (c): $\nu(\mathbf{x})$ and (d): $e_d(\mathbf{x})$.

The governing equation

The interaction terms, Γ_i^P defined in equation (8) and Γ_i^D defined in equation (10) respectively are replaced by their respective expression, and the model partial derivative equation (PDE) (5) becomes:

$$\begin{aligned} \partial_t f_i(t, \mathbf{x}) + \mathbf{v}_i \cdot \partial_{\mathbf{x}} f_i(t, \mathbf{x}) = & \mu[\rho(t, \mathbf{x})] \left(\sum_{h=1}^n P_h(i) f_h(t, \mathbf{x}) - f_i(t, \mathbf{x}) \right) \\ & + \sum_{h=1}^n \sum_{k=1}^n \int_V \eta[\rho(t, \mathbf{x}^*)] B_{hk}(i) [\rho(t, \mathbf{x}^*)] f_h(t, \mathbf{x}) f_k(t, \mathbf{x}^*) d\mathbf{x}^* - f_i(t, \mathbf{x}) \sum_{h=1}^n \int_V \eta[\rho(t, \mathbf{x}^*)] f_h(t, \mathbf{x}^*) d\mathbf{x}^*. \end{aligned} \quad (15)$$

The initial conditions expressed as:

$$f_i(t = t_0, \mathbf{x}) = \phi_i(\mathbf{x}) \quad i = 1, \dots, n, \quad \mathbf{x} \in \Omega, \quad (16)$$

are finally added to the previous PDE (15). After introducing security zones for pedestrians ("pedestrian-wall"), the boundary conditions come from the interactions between pedestrians and the area; therefore, they are included in the management of the interactions.

2.5. Method of characteristics

The method of characteristics is particularly well adapted for solving linear hyperbolic problems and more precisely the transport PDE. Thus we propose to transform the system of equations (15) and (16) from partial differential equations (PDE) to ordinary differential equations (ODE), using the characteristics concept. Indeed, let us consider the characteristic curves associated to the problem defined by equations (15) and (16):

$$\mathbf{X}(t) = (\mathbf{X}_1(t), \mathbf{X}_2(t))^T = (x + t v \cos(\theta_i), y + t v \sin(\theta_i))^T,$$

which is a solution of the following system:

$$\begin{cases} \frac{d\mathbf{X}(t)}{dt} = \mathbf{V}_i, \\ \mathbf{X}(0) = (x, y)^T, \end{cases} \quad (17)$$

where: $\mathbf{V}_i = (v \cos(\theta_i), v \sin(\theta_i))^T$.

Along these curves, the solution of the system defined by equations (15) and (16) satisfies the following system of ODEs :

$$\begin{cases} \frac{d\hat{f}_i(t, \mathbf{x})}{dt} = \hat{\Gamma}_i[f, f](t, \mathbf{x}), \\ \hat{f}_i(0, \mathbf{x}) = \phi_i(\mathbf{x}) \quad \mathbf{x} \in \Omega, \end{cases} \quad \text{for } i = 1, \dots, n, \quad (18)$$

where:

$\hat{f}_i(t, \mathbf{x}) = f_i(t, \mathbf{X}(t)) = f_i(t, x + v \cos(\theta_i)t, y + v \sin(\theta_i)t)$ is the value of f along the characteristics, and

$$\hat{\Gamma}_i[f, f](t, \mathbf{x}) = \hat{\Lambda}_i[f](t, \mathbf{x}) - \mu[\rho(t, \mathbf{x})] \hat{f}_i(t, \mathbf{x}) + \hat{\Psi}_i[f, f](t, \mathbf{x}) - \hat{\Upsilon}_i[f](t, \mathbf{x}) \hat{f}_i(t, \mathbf{x}),$$

where the operators $\hat{\Lambda}$, $\hat{\Psi}$ and $\hat{\Upsilon}$ are defined for $i = 1, \dots, n$ by:

$$\hat{\Lambda}_i[f](t, \mathbf{x}) = \mu[\rho(t, \mathbf{x})] \sum_{h=1}^n P_h(i) f_h(t, x + v (\cos(\theta_i) - \cos(\theta_h))t, y + v (\sin(\theta_i) - \sin(\theta_h))t),$$

$$\widehat{\Psi}_i[f, f](t, \mathbf{x}) = \sum_{h=1}^n \sum_{k=1}^n \int_V \eta[\rho(t, \mathbf{x}^*)] B_{hk}(i) [\rho(t, \mathbf{x}^*)] f_h(t, x + v(\cos(\theta_i) - \cos(\theta_h))t, y + v(\sin(\theta_i) - \sin(\theta_h))t) \\ \times f_k(t, x^* - v\cos(\theta_k)t, y^* - v\sin(\theta_k)t) d\mathbf{x}^*,$$

and finally,

$$\widehat{\Upsilon}_i[f](t, \mathbf{x}) = \sum_{h=1}^n \int_V \eta[\rho(t, \mathbf{x}^*)] f_h(t, x^* - v\cos(\theta_h)t, y^* - v\sin(\theta_h)t) d\mathbf{x}^*.$$

3. Existence and uniqueness of the model solution

This section is devoted to demonstrating proof of the existence and uniqueness of the model solution (18). A first proof of existence and uniqueness was done in [8, 15], in a connected domain without obstacles and border walls. Here, an explicit mathematical proof of the model (18) is proposed expressing the crowd's motion in a bounded domain containing obstacles (the same model as in [8], but with a different second member).

To demonstrate the existence and uniqueness of the solution to problems (18), we relied on the proof given in [8]. Indeed it will be proceeded as follows:

1. Introducing the “mild” solution of the new system of ODE (18).
2. Using the Banach fixed point theorem, the existence and the uniqueness of a “mild” solution is then proven.

185 **First step:**

We introduce the “mild” form of the system (18) obtained by integration along the characteristics, for $i = 1, \dots, n$,

$$\widehat{f}_i(t, \mathbf{x}) = \phi_i(\mathbf{x}) + \int_0^t \widehat{\Lambda}_i[f](s, \mathbf{x}) - \mu[\rho(s, \mathbf{x})] \widehat{f}_i(s, \mathbf{x}) + \widehat{\Psi}_i[f, f](s, \mathbf{x}) - \widehat{\Upsilon}_i[f](s, \mathbf{x}) \widehat{f}_i(s, \mathbf{x}) ds. \quad (19)$$

Second step, choice of the Banach space:

For a given time t , the functional space defined by:

$$\mathbb{L}_n^1(\Omega) = \left\{ \mathbf{f}(t) = (f_1(t), \dots, f_i(t), \dots, f_n(t))^T, \quad \|\mathbf{f}(t)\|_1 = \sum_{i=1}^n \int_{\Omega} |f_i(t, \mathbf{x})| d\mathbf{x} < \infty \right\},$$

is considered.

For a time $T > 0$, let us note the Banach space $\mathbb{X}_T = \mathcal{C}([0, T], \mathbb{L}_n^1(\Omega))$, with the norm: $\|\mathbf{f}\|_{\mathbb{X}_T} = \sup_{t \in [0, T]} \|\mathbf{f}(t)\|_1$.

The following assumptions are then considered :

(A.1.): for all positive real $R > 0$ satisfying $0 < \rho < R$, there exist two constants $c_\mu > 0$ and $c_\eta > 0$ such that:

$$\begin{aligned} 0 < \mu(\rho) < c_\mu, \\ 0 < \eta(\rho) < c_\eta. \end{aligned} \quad (20)$$

(A.2.): $\mu(\rho)$, $\eta(\rho)$ and $B_{hk}(\rho)$ are Lipschitz functions with respect to the density ρ ; namely there are constants L_μ , L_η , L_B such that:

$$\begin{cases} |\mu[\rho_1] - \mu[\rho_2]| \leq L_\mu |\rho_1 - \rho_2|, & 0 < \rho_1 < R, \quad 0 < \rho_2 < R, \\ |\eta[\rho_1] - \eta[\rho_2]| \leq L_\eta |\rho_1 - \rho_2|, & 0 < \rho_1 < R, \quad 0 < \rho_2 < R, \\ |B_{hk}(i)[\rho_1] - B_{hk}(i)[\rho_2]| \leq L_B |\rho_1 - \rho_2|, & i, h, k = 1, \dots, n. \end{cases} \quad (21)$$

The main two theorems for the local and global existence, respectively are given in the following:

Theorem 1. (*Local existence*)

Let $\phi = (\phi_1, \dots, \phi_i, \dots, \phi_n)^T \in \mathbb{L}_n^\infty(\Omega)$ with $\phi \geq 0$, there exists φ^0 , a time $T > 0$ and two constants a_0 , R , such that if $\|\phi\|_1 \leq \varphi^0$, the problem (18) has a unique positive solution $\mathbf{f} = (f_1, \dots, f_i, \dots, f_n)^T \in \mathbb{X}_T$, satisfying:

$$\|\mathbf{f}\|_{\mathbb{X}_T} \leq a_0 \|\phi\|_1,$$

$$\rho(t, \mathbf{x}) \leq R, \quad \forall t \in [0, T], \quad \forall \mathbf{x} \in \Omega.$$

Moreover, if

$$\sum_{i=1}^n \|\phi_i\|_\infty \leq 1, \quad (22)$$

we have:

$$\rho(t, \mathbf{x}) \leq 1, \quad \forall t \in [0, T], \quad \forall \mathbf{x} \in \Omega. \quad (23)$$

Theorem 2. (*Global existence*)

Considering the same assumptions as in Theorem 1, there exists φ^p , ($p = 1, \dots, m-1, m \in \mathbb{N}$), a_p , ($p = 1, \dots, m-1, m \in \mathbb{N}$), such that if $\|\phi\|_1 \leq \varphi^p$, the problem (18) has a unique maximum positive solution $\mathbf{f} \in \mathcal{C}([0, (m-1)T], \mathbb{L}_n^1(\Omega))$, satisfying for any $p \leq m-1$,

$$\sup_t \|\mathbf{f}(t + (p-1)T)\|_1 \leq a_{p-1} \|\phi\|_1, \quad t \in [0, T],$$

$$\rho(t + (p-1)T, \mathbf{x}) \leq R, \quad \forall t \in [0, T], \quad \forall \mathbf{x} \in \Omega.$$

In addition, if ϕ satisfies (22), we have:

$$\rho(t + (p-1)T, \mathbf{x}) \leq 1, \quad \forall t \in [0, T], \quad \forall \mathbf{x} \in \Omega.$$

Proof of Theorem 1

The following function:

$$\psi_i(t, \mathbf{x}) = f_i(t, \mathbf{x}) \exp(\lambda t) \quad \text{for } i = 1, \dots, n, \quad \lambda > 0,$$

is first introduced. The system (18) is equivalent to the following system:

$$\begin{cases} \frac{d\widehat{\psi}_i(t, \mathbf{x})}{dt} = \lambda \widehat{\psi}_i(t, \mathbf{x}) + \widehat{\Lambda}_i[\psi](t, \mathbf{x}) - \widehat{\psi}_i \mu[\rho(t, \mathbf{x})] + \exp(-\lambda t) [\widehat{\Psi}_i[\psi, \psi](t, \mathbf{x}) - \widehat{\Upsilon}_i[\psi](t, \mathbf{x}) \widehat{\psi}_i], \\ \widehat{\psi}_i(0, \mathbf{x}) = \phi_i(\mathbf{x}) \quad \mathbf{x} \in \Omega \quad \text{for } i = 1, \dots, n. \end{cases} \quad (24)$$

For all $t \in [0, T]$, we integrate (24). Then, the following ‘‘mild’’ formulation, is deduced:

$$\widehat{\psi}_i(t, \mathbf{x}) = \phi_i(\mathbf{x}) + \int_0^t \left[\exp(-\lambda s) \widehat{\Psi}_i[\psi, \psi](s, \mathbf{x}) + \widehat{\Lambda}_i[\psi](s, \mathbf{x}) + (\lambda - \mu[\rho(s, \mathbf{x}) - \widehat{\Upsilon}_i[\psi](s, \mathbf{x}) \exp(-\lambda s)]) \widehat{\psi}_i(s, \mathbf{x}) \right] ds. \quad (25)$$

Let us consider the operator $\mathbf{A} = (\widehat{A(\psi)})_1, \dots, \widehat{A(\psi)}_i, \dots, \widehat{A(\psi)}_n)^T$, and its i -th component defined by:

$$\widehat{A(\psi)}_i(t, \mathbf{x}) = \phi_i(\mathbf{x}) + \int_0^t \left[\exp(-\lambda s) \widehat{\Psi}_i[\psi, \psi](s, \mathbf{x}) + \widehat{\Lambda}_i[\psi](s, \mathbf{x}) + (\lambda - \mu[\rho(s, \mathbf{x}) - \widehat{\Upsilon}_i[\psi](s, \mathbf{x}) \exp(-\lambda s)]) \widehat{\psi}_i(s, \mathbf{x}) \right] ds. \quad (26)$$

To show that the system (24) has a solution, it is sufficient to show that the operator \mathbf{A} has a unique fixed point in the Banach space \mathbb{X}_T . Indeed, let us introduce the set defined by:

$$B_{T, a_0, \lambda, R} = \left\{ \boldsymbol{\psi} = (\psi_1, \dots, \psi_i, \dots, \psi_n)^T \in \mathbb{X}_T : \psi_i \geq 0, \quad \|\boldsymbol{\psi}\|_{\mathbb{X}_T} \leq a_0 \|\boldsymbol{\phi}\|_1, \right. \\ \left. \sum_{i=1}^n \psi_i(t, x - v \cos(\theta_i)t, y - v \sin(\theta_i)t) \leq R \exp(\lambda t), \quad t \in [0, T], \quad \mathbf{x} \in \Omega \right\}.$$

The operator \mathbf{A} has a unique fixed point if the following two properties are satisfied:

- (P.1) Let $\boldsymbol{\psi} \in B_{T, a_0, \lambda, R}$ then, $\mathbf{A}\boldsymbol{\psi} \in B_{T, a_0, \lambda, R}$.
- (P.2) The application $\mathbf{A} : B_{T, a_0, \lambda, R} \rightarrow B_{T, a_0, \lambda, R}$ is a contraction.

In what follows, the constants T, a_0, λ, R , must be chosen carefully in order to obtain properties (P.1) and (P.2).

The proof of both properties (P.1) and (P.2) is based on the following Lemma:

Lemma 1. *Let $T > 0$, $\lambda > 0$, $\boldsymbol{\psi}^1 = (\psi_1^1, \dots, \psi_i^1, \dots, \psi_n^1)^T \in \mathbb{X}_T$ and $\boldsymbol{\psi}^2 = (\psi_1^2, \dots, \psi_i^2, \dots, \psi_n^2)^T \in \mathbb{X}_T$ such that :*

$$\sum_{i=1}^n \psi_i^j(t, x - v \cos(\theta_i)t, y - v \sin(\theta_i)t) \leq R \exp(\lambda t) \quad t \in [0, T], \quad \mathbf{x} \in \Omega \quad \text{for } j = 1, 2, \lambda > 0, R > 0. \quad (27)$$

Then,

1. There are $C_1 > 0$, $C_2 > 0$ such that,

$$\|\mathbf{A}\boldsymbol{\psi}^1 - \mathbf{A}\boldsymbol{\psi}^2\|_{\mathbb{X}_T} \leq \left[\frac{C_1}{\lambda} (\|\boldsymbol{\psi}^1\|_{\mathbb{X}_T} + \|\boldsymbol{\psi}^2\|_{\mathbb{X}_T}) + (\lambda + C_2) T \right] \|\boldsymbol{\psi}^1 - \boldsymbol{\psi}^2\|_{\mathbb{X}_T}, \quad (28)$$

where:

$$C_1 = 2c_\eta + R(nc_\eta L_B + (n+1)L_\eta), \\ C_2 = 2c_\mu + (n+1)RL_\mu. \quad (29)$$

2. If $\psi_i(t, \mathbf{x}) \geq 0$ and $\phi_i(\mathbf{x}) \geq 0$ then, there exists λ_0 such that: $(\widehat{A\psi})_i(t, \mathbf{x}) \geq 0$ for all $t \in [0, T]$, $\mathbf{x} \in \Omega$ and $\lambda \geq \lambda_0$, $i = 1, \dots, n$,

where:

$$\lambda_0 = Rc_\eta |V| + c_\mu, \\ |V|: \text{ is the measure of visibility zone } V, \quad |V| = \int_V d\mathbf{x}. \quad (30)$$

3. There exist R_1 and T such that, for all $R \geq R_1$ and $t \leq T$, we get:

$$\sum_{i=1}^n (A\psi)_i(t, x - v \cos(\theta_i)t, y - v \sin(\theta_i)t) \leq R \exp(\lambda t) \quad t \in [0, T_0], \quad \mathbf{x} \in \Omega. \quad (31)$$

where:

$$R_1 = \sum_{i=1}^n \|\phi_i\|_\infty, \quad (32)$$

$$T = \frac{1}{\lambda} \ln \left(1 + \frac{\lambda}{nR(c_\eta R|V| + c_\mu)} \left(R - \sum_{i=1}^n \|\phi_i\|_\infty \right) \right) := T_0. \quad (33)$$

4.

$$\|\mathbf{A}\psi\|_{\mathbb{X}_T} \leq \|\phi\|_1 + \frac{C_1}{\lambda} \|\psi\|_{\mathbb{X}_T}^2 + (\lambda + C_2) T \|\psi\|_{\mathbb{X}_T}. \quad (34)$$

The proof of this Lemma is given in Appendix A.

Let $\psi^1, \psi^2 \in B_{T, a_0, \lambda, R}$, and T be defined by:

$$T = \frac{1}{C_2 + \lambda} T_0 \leq T_0, \quad (35)$$

where T_0 is the expression of time defined in equation (33), and C_2 is defined in equation (29).

According to the inequality (34),

$$\|\mathbf{A}\psi\|_{\mathbb{X}_T} \leq \|\phi\|_1 + \frac{C_1}{\lambda} \|\psi\|_{\mathbb{X}_T}^2 + (\lambda + C_2) T \|\psi\|_{\mathbb{X}_T}, \quad (36)$$

since $\psi \in B_{T, a_0, \lambda, R}$; we have $\|\psi\|_{\mathbb{X}_T} \leq a_0 \|\phi\|_1$, moreover,

$$\|\mathbf{A}\psi\|_{\mathbb{X}_T} \leq \|\phi\|_1 + \frac{1}{\lambda} C_1 a_0^2 \|\phi\|_1^2 + (C_2 + \lambda) T a_0 \|\phi\|_1. \quad (37)$$

Then, $\|\mathbf{A}\psi\|_{\mathbb{X}_T} \leq a_0 \|\phi\|_1$, if a_0 satisfies the following equation:

$$(E_0) : \|\phi\|_1 + \frac{1}{\lambda} C_1 a_0^2 \|\phi\|_1^2 + (C_2 + \lambda) T a_0 \|\phi\|_1 = a_0 \|\phi\|_1.$$

Indeed, the constant a_0 exists if:

$$\|\phi\|_1 \leq \min \left\{ \frac{(n-1)^2 c_\mu}{8n^2 c_\eta}, \frac{(n-1)^2 c_\eta |V|}{(4n^2 (nc_\eta L_B + (n+1)L_\eta))} \right\} := \varphi^0, \quad (\text{for the proof see Appendix B}).$$

which leads to the existence of a_0 if $\|\phi\|_1$ is "small".

In addition, from Lemma 1 for all $\|\phi\|_1 \leq \varphi^0$, $R \geq R_1$, $\lambda = \lambda_0$, $t \leq T \leq T_0$ and a_0 the smallest solution among the two positive solutions of equation (E_0) , where R_1 , λ_0 , and T , are given by (32), (30), (35), respectively, we get:

$$\text{if } \psi \in B_{T, a_0, \lambda, R} \text{ then } \mathbf{A}\psi \in B_{T, a_0, \lambda, R} \quad \forall t \in [0, T].$$

This ends the proof of property (P.1).

On the other hand, from Lemma 1, we have:

$$\|\mathbf{A}\psi^1 - \mathbf{A}\psi^2\|_{\mathbb{X}_T} \leq \left(\frac{2C_1}{\lambda} a_0 \|\phi\|_1 + (C_2 + \lambda) T \right) \|\psi^1 - \psi^2\|_{\mathbb{X}_T}. \quad (38)$$

Let a_0 , the small positive solution of equation (E_0) be defined by:

$$a_0 = \lambda \frac{(1 - (\lambda + C_2)T) - \sqrt{\Delta_0}}{2C_1 \|\phi\|_1}, \quad (39)$$

where Δ_0 is the discriminant of equation (E_0)

$$\Delta_0 = ((C_2 + \lambda)T - 1)^2 - 4 \frac{C_1}{\lambda} \|\phi\|_1. \quad (40)$$

Hence,

$$0 \leq \left(\frac{2C_1}{\lambda} a_0 \|\phi\|_1 + (C_2 + \lambda)T \right) = 1 - \sqrt{\Delta_0} < 1.$$

195 From there, the operator $\mathbf{A} : B_{T,a_0,\lambda,R} \rightarrow B_{T,a_0,\lambda,R}$ is a contraction. This ends the proof of property (P.2).

The fixed point theorem ends the proof of Theorem 1, which refers to local existence.

From the foregoing, there exist φ^0 , λ_0 , T , a_0 and R , such that the problem (18) has a unique positive solution $\mathbf{f} = (f_1, \dots, f_i, \dots, f_n)^T \in \mathbb{X}_T$, satisfying:

$$\rho(t, \mathbf{x}) \leq R, \quad \forall t \in [0, T], \quad \forall \mathbf{x} \in \Omega. \quad \forall R \geq R_1,$$

where

$$R_1 = \sum_{i=1}^n \|\phi_i\|_\infty.$$

Moreover if ϕ satisfies (22) ($R_1 \leq 1$), then one can choose R such that (23) can be obtained; for example, the R can be chosen as:

$$R = \frac{1 + \sum_{i=1}^n \|\phi_i\|_\infty}{2} > R_1. \quad (41)$$

This completes the proof.

Proof of Theorem 2

To prove the existence for large times of the problem's solution (18), it is equivalent to show that the solution obtained by Theorem 1 admits an extension on each interval $[0, pT]$ for $p \in \mathbb{N}$.

Let ϕ satisfying the conditions of Theorem 1. R , $\lambda = \lambda_0$ and T are given by (41), (30), (35), respectively, and are fixed and depending on initial data ϕ .

Consequently, there exists φ^1 such that if $\|\phi\|_1 \leq \varphi^1$, there exists a_1 such that the solution to (18) obtained by Theorem 1 can be extended in the interval $[T, 2T]$ and satisfies the estimates

$$\|\psi(t+T)\|_{\mathbb{X}_T} \leq a_1 \|\phi\|_1, \quad \forall t \in [0, T], \quad (42)$$

$$\rho(t+T, \mathbf{x}) \leq R, \quad \forall t \in [0, T], \quad \forall \mathbf{x} \in \Omega. \quad (43)$$

Indeed, the problem (24) on $[T, 2T]$ with a given initial condition defined by $\psi(T, \mathbf{x})$ can be solved, more precisely $\forall t \in [0, T]$ we have :

$$\begin{aligned} \widehat{\psi}_i(t+T, \mathbf{x}) &= \psi_i(T, \mathbf{x}) + \int_0^t \left[\exp(-\lambda(s+T)) \widehat{\Psi}_i[\psi, \psi](s+T, \mathbf{x}) + \widehat{\Lambda}_i[\psi](s+T, \mathbf{x}) \right. \\ &\quad \left. + (\lambda - \mu[\rho(s+T, \mathbf{x}) - \widehat{\Upsilon}_i[\psi](s+T, \mathbf{x})] \exp(-\lambda(s+T))) \widehat{\psi}_i(s+T, \mathbf{x}) \right] ds, \text{ for } i = 1, \dots, n. \end{aligned}$$

Let us consider the set defined by:

$$B_{T,a_1,\lambda,R} = \left\{ \boldsymbol{\psi}(t+T) = (\psi_1(t+T), \dots, \psi_i(t+T), \dots, \psi_n(t+T))^T \in \mathbb{X}_T : \psi_i \geq 0, \|\boldsymbol{\psi}(t+T)\|_{\mathbb{X}_T} \leq a_1 \|\boldsymbol{\phi}\|_1, \right. \\ \left. \sum_{i=1}^n \psi_i(t+T, x - v \cos(\theta_i)(t+T), y - v \sin(\theta_i)(t+T)) \leq R \exp(\lambda(t+T)) \quad t \in [0, T], \mathbf{x} \in \Omega \right\}.$$

where R, λ, T, a_0 are fixed and depending on initial data $\boldsymbol{\phi}$.

In the same way as in the case of local existence, it can be shown that, for $\boldsymbol{\psi}(t+T) \geq 0$, $t \in [0, T]$, R given by (41), $\lambda = \lambda_0$, and T given by (35), we get :

$$\left(\widehat{A\boldsymbol{\psi}} \right)_i(t+T, \mathbf{x}) \geq 0, \quad i = 1, \dots, n, \quad t \in [0, T], \quad \mathbf{x} \in \Omega,$$

and

$$\sum_{i=1}^n (A\boldsymbol{\psi})_i(t+T, x - v \cos(\theta_i)(t+T), y - v \sin(\theta_i)(t+T)) \leq R \exp(\lambda(t+T)) \quad i = 1, \dots, n, \quad t \in [0, T], \quad \mathbf{x} \in \Omega.$$

In addition, it can be shown that:

$$\|\mathbf{A}\boldsymbol{\psi}(t+T)\|_{\mathbb{X}_T} \leq a_0 \|\boldsymbol{\phi}\|_1 + \frac{1}{\lambda} C_1 a_1^2 \|\boldsymbol{\phi}\|_1^2 + (C_2 + \lambda) T a_1 \|\boldsymbol{\phi}\|_1. \quad (44)$$

Then, $\|\mathbf{A}\boldsymbol{\psi}(t+T)\|_{\mathbb{X}_T} \leq a_1 \|\boldsymbol{\phi}\|_1$, if a_1 satisfies the following equation:

$$(E_1) : a_0 \|\boldsymbol{\phi}\|_1 + \frac{1}{\lambda} C_1 a_1^2 \|\boldsymbol{\phi}\|_1^2 + (C_2 + \lambda) T a_1 \|\boldsymbol{\phi}\|_1 = a_1 \|\boldsymbol{\phi}\|_1.$$

Moreover, there exists a solution of equation (E_1) in a_1 if its discriminant $\Delta_1 = ((C_2 + \lambda)T - 1)^2 - 4 \frac{C_1}{\lambda} a_0 \|\boldsymbol{\phi}\|_1$ is positive.

With a choice of $\boldsymbol{\phi}$ such that: $\|\boldsymbol{\phi}\|_1 \leq \min \left(\varphi^0, \lambda \frac{((C_2 + \lambda)T - 1)^2}{4C_1 a_0} \right) := \varphi^1$, we have: $\Delta_1 \geq 0$.

From there, for $\|\boldsymbol{\phi}\|_1 \leq \varphi^1$, $t \in [0, T]$ with T is given by (35), R given by (41), a_1 is a positive solution of equation (E_1) , we have:

$$\text{if } \boldsymbol{\psi}(t+T) \in B_{T,a_1,\lambda,R} \text{ then } \mathbf{A}\boldsymbol{\psi}(t+T) \in B_{T,a_1,\lambda,R} \quad \forall t \in [0, T].$$

In addition, let $\boldsymbol{\psi}_1(t+T), \boldsymbol{\psi}_2(t+T) \in B_{T,a_1,\lambda,R}$, then:

$$\|\mathbf{A}\boldsymbol{\psi}_1(t+T) - \mathbf{A}\boldsymbol{\psi}_2(t+T)\|_{\mathbb{X}_T} \leq \left(\frac{2C_1}{\lambda} a_1 \|\boldsymbol{\phi}\|_1 + (C_2 + \lambda) T \right) \|\boldsymbol{\psi}_1(t+T) - \boldsymbol{\psi}_2(t+T)\|_{\mathbb{X}_T}. \quad (45)$$

Let us consider a_1 the smallest solution among the two positive solutions of the equation (E_1) , given by: $a_1 = \lambda \frac{(1 - (\lambda + C_2)T) - \sqrt{\Delta_1}}{2C_1 \|\boldsymbol{\phi}\|_1} \geq 0$,

since

$$0 \leq \left(\frac{2C_1}{\lambda} a_1 \|\boldsymbol{\phi}\|_1 + (C_2 + \lambda) T \right) = 1 - \sqrt{\Delta_1} < 1.$$

By applying the fixed point theorem which gives the existence and uniqueness of solution $\boldsymbol{\psi}(t+T) \in \mathbb{X}_T$, more precisely existence of a solution in $[T, 2T]$. This solution is continuous in $[T, 2T]$ and, in particular, it satisfies (42) and (43). Moreover, if $\boldsymbol{\phi}$ satisfies (22) ($\sum_{i=1}^n \|\phi_i\|_\infty \leq 1$), for R given by (41), we have,

$$\rho(t, \mathbf{x}) \leq 1, \quad \forall t \in [T, 2T], \quad \forall \mathbf{x} \in \Omega.$$

The iteration process can be applied to prove the existence for large times. Suppose that the solution exists and is continuous in $[0, (m-1)T]$ and satisfies: $\|\psi(t + (p-1)T)\|_{\mathbb{X}_T} \leq a_{p-1}\|\phi\|_1$, for $p = 1, \dots, m$, $t \in [0, T]$, $\|\psi(pT)\|_{\mathbb{X}_T} \leq a_{p-1}\|\phi\|_1$, for $p = 1, \dots, m$, and $\rho(t + (p-1)T, \mathbf{x}) \leq R$, for $p = 1, \dots, m$, $t \in [0, T]$ $\mathbf{x} \in \Omega$. where, $a_0, \Delta_0, R, \lambda, T$ are given by (39), (40), (41), (30), (35) respectively.

a_p and Δ_p for $p = 1, \dots, m-1$ are given by:

$$a_p = \lambda \frac{(1 - (\lambda + C_2)T) - \sqrt{\Delta_p}}{2C_1\|\phi\|_1},$$

$$\Delta_p = ((C_2 + \lambda)T - 1)^2 - 4\frac{C_1}{\lambda}a_{p-1}\|\phi\|_1.$$

It can now be proved that we can extend the solution in $[(m-1)T, mT]$, satisfying the following inequality:

$$\|\psi(t + (m-1)T)\|_1 \leq a_{m-1}\|\phi\|_1, \quad t \in [0, T], \quad (46)$$

$$\|\psi(mT)\|_1 \leq a_{m-1}\|\phi\|_1, \quad (47)$$

$$\rho(t + (m-1)T, \mathbf{x}) \leq R, \quad t \in [0, T] \quad \mathbf{x} \in \Omega. \quad (48)$$

Let $\psi = (\psi_i)_{i=1, \dots, n}$ be the solution of the following problem, for $i = 1, \dots, n$

$$\begin{aligned} \widehat{\psi}_i(t + (m-1)T, \mathbf{x}) &= \widehat{\psi}_i((m-1)T, \mathbf{x}) + \int_{(m-1)T}^{t+(m-1)T} \left[\exp(-\lambda(s)) \widehat{\Psi}_i[\psi, \psi](s, \mathbf{x}) + \widehat{\Lambda}_i[\psi](s, \mathbf{x}) \right. \\ &\quad \left. + (\lambda - \mu[\rho(s, \mathbf{x}) - \widehat{\Upsilon}_i[\psi](s, \mathbf{x}) \exp(-\lambda(s))]) \widehat{\psi}_i(s, \mathbf{x}) \right] ds. \end{aligned}$$

In the same way as in the case of local existence, it can be shown that:

$$\|\mathbf{A}\psi(t + (m-1)T)\|_{\mathbb{X}_T} \leq a_{m-2}\|\phi\|_1 + \frac{1}{\lambda}C_1a_{m-1}^2\|\phi\|_1^2 + (C_2 + \lambda)Ta_{m-1}\|\phi\|_1,$$

$$\|\mathbf{A}\psi^1(t + (m-1)T) - \mathbf{A}\psi^2(t + (m-1)T)\|_{\mathbb{X}_T} \leq \left(\frac{2C_1}{\lambda}a_{m-1}\|\phi\|_1 + (C_2 + \lambda)T \right) \|\psi^1(t + (m-1)T) - \psi^2(t + (m-1)T)\|_1$$

If we choose a_{m-1} so that,

$$a_{m-1} = \lambda \frac{(1 - (\lambda + C_2)T) - \sqrt{\Delta_{m-1}}}{2C_1\|\phi\|_1}, \quad (49)$$

where,

$$\Delta_{m-1} = ((C_2 + \lambda)T - 1)^2 - 4\frac{C_1}{\lambda}a_{m-2}\|\phi\|_1. \quad (50)$$

Then a_{m-1} is a solution of

$$(E_{m-1}) : \|\phi\|_1 + \frac{1}{\lambda}C_1a_{m-1}^2\|\phi\|_1^2 + (C_2 + \lambda)Ta_{m-1}\|\phi\|_1 = a_{m-1}\|\phi\|_1.$$

Moreover

$$0 \leq \left(\frac{2C_1}{\lambda}a_{m-1}\|\phi\|_1 + (C_2 + \lambda)T \right) = 1 - \sqrt{\Delta_{m-1}} < 1,$$

which gives the solution in $[(m-1)T, mT]$, satisfying (46)-(48). Moreover, if ϕ satisfies (22) ($\sum_{i=1}^n \|\phi_i\|_\infty \leq 1$), for R given by (41), we have:

$$\rho(t, \mathbf{x}) \leq 1, \quad \forall t \in [(m-1)T, mT], \quad \forall \mathbf{x} \in \Omega.$$

200 This completes the proof of Theorem 2.

4. Simulations

4.1. Numerical method

The numerical method used in this work is the same numerical scheme described in [7, 8], is based on the so called splitting method [20] to solve the proposed mathematical model defined by:

$$\begin{cases} \partial_t f_i(t, \mathbf{x}) + \mathbf{v}_i \cdot \partial_{\mathbf{x}} f_i(t, \mathbf{x}) = \Gamma_i[f](t, \mathbf{x}) & i = 1, \dots, n, \quad t \in [0, T], \\ f_i(0, \mathbf{x}) = \phi_i(\mathbf{x}) & i = 1, \dots, n, \quad \mathbf{x} \in \Omega, \end{cases} \quad (51)$$

on an interval of time $[0, T]$. The principle of the method consists in introducing a subdivision $[t_k]_{k=0, \dots, T}$ of the interval $[0, T]$, and solving on each subdivision $[t_k, t_{k+1}]$ the two following systems:

$$\begin{cases} \partial_t \widehat{f}_i(t, \mathbf{x}) + \mathbf{v}_i \cdot \partial_{\mathbf{x}} \widehat{f}_i(t, \mathbf{x}) = 0 & i = 1, \dots, n, \quad t \in [t_k, t_{k+\frac{1}{2}}], \\ \widehat{f}_i(0, \mathbf{x}) = \phi_i(\mathbf{x}) & i = 1, \dots, n, \quad \mathbf{x} \in \Omega, \end{cases} \quad (52)$$

where $\phi_i(\mathbf{x})$ is the initial distribution of pedestrians, and

$$\begin{cases} \partial_t f_i(t, \mathbf{x}) = \Gamma_i[f](t, \mathbf{x}) & i = 1, \dots, n, \quad t \in [t_{k+\frac{1}{2}}, t_{k+1}], \\ f_i(0, \mathbf{x}) = \widehat{f}_i(\mathbf{x}) & i = 1, \dots, n, \quad \mathbf{x} \in \Omega, \end{cases} \quad (53)$$

where $\widehat{f}_i(\mathbf{x})$ is the solution of system (52).

For the resolution of the transport equation (52), the upwind scheme of order 1 [21, 22] is used, and for the ordinary differential equation (53), Euler's method of order 1 is preferred.

4.2. Numerical results and application to the evacuation of a room

Several authors [1] reported that an obstacle can either facilitate or obstruct pedestrian evacuation of a room with an exit, depending on its position, size and shape. In particular it has been shown that an obstacle may have a strong influence on pedestrians if it is located close to the exit.

In order to show the performance of the proposed mathematical model, it has been applied to the evacuation of a room with and without an obstacle and our study is restricted to the mathematical model without taking into account the internal interactions between the pedestrians. This choice is motivated by considering a small number of pedestrians ($N \leq 50$ pedestrians). Our goal is to study the influence of an obstacle on evacuation time and describe some characteristics of the dynamics of a crowd in a bounded domain (with walls, size of the exit and dimensions of the obstacle) namely, avoidance and evacuation.

Therefore the mathematical model (51) becomes:

$$\begin{cases} \partial_t f_i(t, \mathbf{x}) + \mathbf{v}_i \cdot \partial_{\mathbf{x}} f_i(t, \mathbf{x}) = \Gamma_i^D[f](t, \mathbf{x}) & i = 1, \dots, n, \quad t \in [0, T], \\ f_i(0, \mathbf{x}) = \phi_i(\mathbf{x}) & i = 1, \dots, n, \quad \mathbf{x} \in \Omega. \end{cases} \quad (54)$$

It is assumed here that $\sigma = 1$ and the velocity has a constant modulus. Moreover pedestrians can take nine directions, and 9 densities: $f_i(t, \mathbf{x}) = f(t, \mathbf{x}, \theta_i)$, $i = 1, \dots, 9$ (see fig. 8), are taken into account.

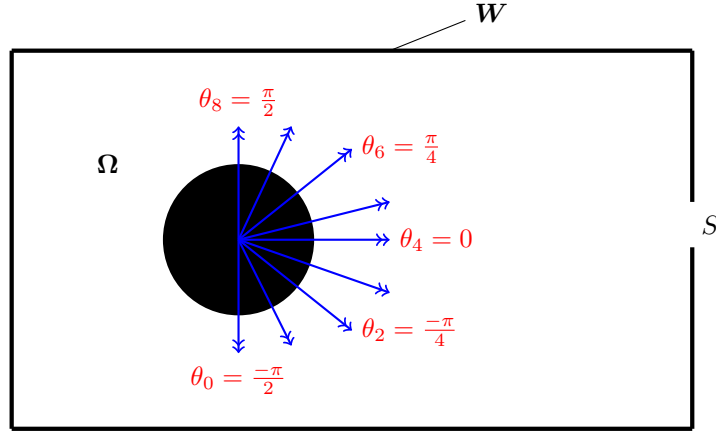


Figure 8: Illustration of the nine directions defined by: $\theta_k = \frac{k-4}{8}\pi : k = 0, \dots, 8$, that each pedestrian can take.

For all the simulations, the following parameters are chosen:

- dimensions of the domain: length $L_x = 11m$, and width $L_y = 11m$.
- size of exit: $S = 1.5m$.
- quality of domain: $\alpha = 1$.
- 9 different directions of velocity on the set S_θ ,

$$S_\theta = \left\{ \theta_i = \frac{i-4}{8}\pi : i = 0, \dots, 8 \right\}.$$

- rate of interactions: $\mu = 1 - \rho$, with $0 < \mu < 1$.

220 The dimensionless quantities are obtained with reference to the following reference variables: $L = 11\sqrt{2} m$, $V_m = 2 m.s^{-1}$, $T_m = 7.78 s$.

A value of $\rho_{max} = 7$ pedestrians / m^2 is chosen to normalize the local density, which is a high value.

225 The first application deals with the evacuation of $N = 50$ people of a room, first without obstacle and then with an obstacle. This group of 50 pedestrians at initial time is gathered in a circular area of radius $r = 1.91m$. The maximum number of pedestrians $N_{max} = 7\pi r^2 = 80$. The normalized local density at the initial time (within a circular area) is: $\rho_0 = \frac{50}{\pi r^2 \rho_{max}} = 0.62$. Three cases are considered: first without any obstacle, second with a fixed square-shaped obstacle located between the center of the disk \mathcal{D}_0 and the exit and last with a fixed square-shaped obstacle just in front of the exit. For the two last cases, the dimensions of the obstacle are identical :
230 $L_{obs} = l_{obs} = 1.5m$.

The second application concerns the comparison of the evacuation time obtained by our technique and that obtained by a deterministic discrete method in the simple case of the evacuation of a room without obstacle. The evacuation time is defined as the time when the last pedestrian has left the room. Finally, an obstacle is introduced in the room
235 and the last application examines the effect of the dimensions and location of an obstacle on the time evacuation.

4.2.1. Evacuation of a room without obstacle and with a fixed obstacle

In the first case of the room without obstacle, the coordinates of the center of the disk \mathcal{D}_0 at $t = 0$ are $M_0 = (2.3; 3)$; and the results of our model, obtained at four successive times are illustrated in Figures 9a, b, c and d.

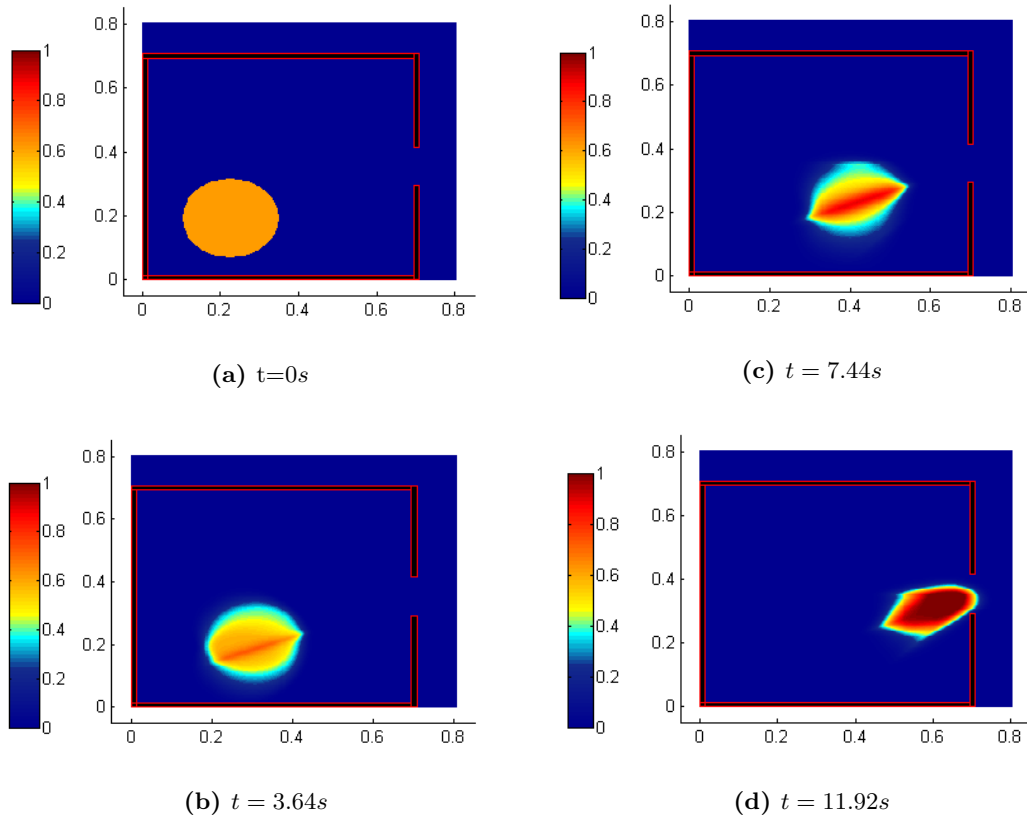


Figure 9: Time evolution of the local pedestrians density at different times: (a): $t = 0s$, (b): $t = 3.64s$, (c): $t = 7.44s$, and (d): $t = 11.92s$.

In the second case, the room contains a fixed square-shaped obstacle (1) whose lower left corner has the coordinates (6.;2.2), and the center of the initial disk is: \mathcal{D}_0 is: $M_0 = (2.3; 2.5)$. The results obtained by our model at four different times are then illustrated in Figures 10 a, b, c and d.

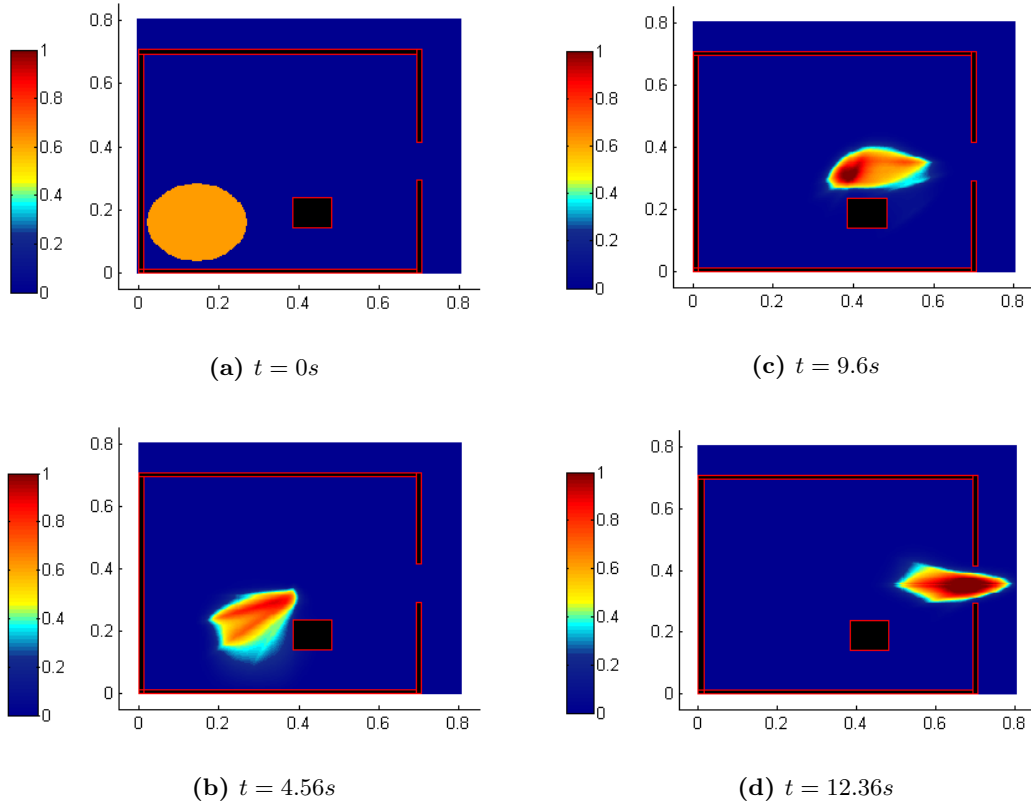


Figure 10: Time evolution of the local pedestrians density at 4 different times: (a): $t = 0s$, (b): $t = 4.56s$, (c): $t = 9.6s$, and (d): $t = 12.36s$.

In the last case, the obstacle (2) whose lower left corner located at the left bottom has the coordinates $(6.25; 4.75)$, is located in front of the exit at a distance of $3.5m$. The center of the initial disk \mathcal{D}_0 is: $M_0 = (2.3; 5.5)$. The results obtained from the proposed procedure at six different times are illustrated in Figures 11 a, b, c, d, e and f.

245 The group of pedestrians splits into two subgroups when in front of the obstacle to avoid it and with the obstacle bypassed, the group reforms when it leaves the room.

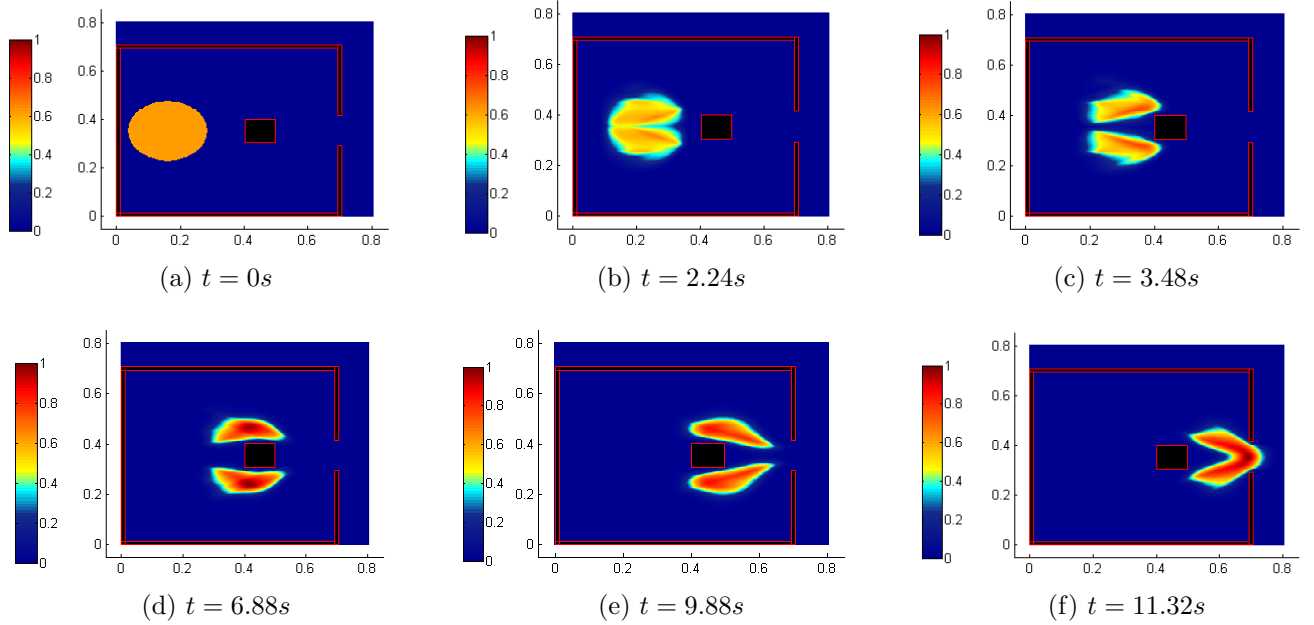


Figure 11: Time evolution of the local pedestrians density, (a): $t = 0s$, (b): $t = 2.24s$, (c): $t = 3.48s$, (d): $t = 6.88s$, (e): $t = 9.88s$ and (f): $t = 11.32s$.

Finally, the evacuation time is collected for the three cases in Tab. (3). It can be noted that the evacuation time is slightly improved when the obstacle (2) is located in front of the exit.

without obstacle	with obstacle (1)	with obstacle (2)
12.6 s	13.41 s	12.59 s

Table 3: Evacuation time (s).

250 4.2.2. Comparison of the proposed method with deterministic approach

In order to check the validity of the proposed kinetic model, the evacuation time for a room without obstacle calculated with our kinetic model is compared with a mean evacuation time obtained by a discrete deterministic model: CAPFlow developed by Argoul et al. [3]. In CAPFlow simulations, the pedestrians are randomly distributed in a circular area of radius $r = 1.91m$. Let the density ρ be in $[1.3 \ 4.3]$ pedestrians/ m^2 . To examine the sensitivity
 255 of the deterministic model to changes in the value of model parameters, the value of some parameters are changed in a random manner (normal law): the radii of the disks representing the pedestrians, the relaxation time after a collision to recover the desired direction etc [1]. 150 simulations with the CAPFlow model are performed. The evacuation time taken by the pedestrians to reach the exit is calculated by both the kinetic and discrete models and the results for four local pedestrians densities are shown in Table 4.

Initial density (pedestrian/ m^2)	Normalized local density ρ_0	Number of pedestrians N	Kinetic model Evacuation time (s)	Discrete model Mean evacuation time (s)
1.3	0.18	15	11.12	11.10
2.6	0.37	30	11.46	11.51
3.4	0.49	40	11.62	11.67
4.3	0.62	50	11.78	11.80

Table 4: Evacuation time calculated by the kinetic and discrete models for four initial densities.

According to the results in the previous table, the evacuation times obtained by the kinetic and discrete models, respectively, for each case are very similar.

4.2.3. Influence of the obstacle's position and dimensions on the evacuation time

A fixed obstacle in a room is now located in front of the exit (see fig.12). As previously a group of $N = 50$ pedestrians evacuates the room. Our goal is to study the influence of the obstacle on the evacuation time of the group.

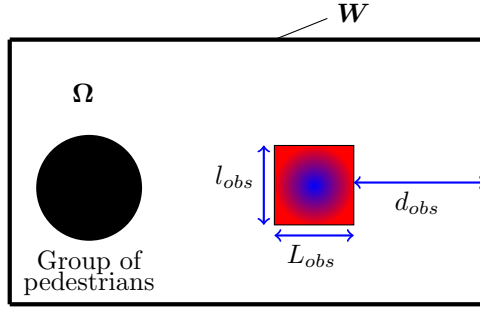


Figure 12: Illustration of the obstacle characteristics : L_{obs}, l_{obs} are its dimensions, and d_{obs} the distance between the exit and the obstacle.

The group of $N = 50$ pedestrians is distributed in a circular area of radius $r = 1.91m$ in an empty room (without obstacle). The normed local density at the initial circular area is as previously: $\rho = \frac{50}{\pi r^2 \rho_m} = 0.62$. The evacuation time computed by our technique, to leave the room without any obstacle is: 11.78s.

Then, the obstacle is located in the room, and the obstacle's dimensions and their distance to the exit are changed. Then, the evacuation time is performed, and its values are collected in Table 5.

d_{obs} (m)	$L_{obs} \times l_{obs}$ ($m \times m$)	Evacuation time (s)
1.5	0.5×0.5	12.36
	0.75×0.75	12.48
	1×1	12.20
	1.25×1.25	12.00
	1.5×1.5	12.62
1.75	0.5×0.5	12.32
	0.75×0.75	12.42
	1×1	11.86
	1.25×1.25	11.42
	1.5×1.5	11.48
2	0.5×0.5	12.28
	0.75×0.75	12.38
	1×1	11.78
	1.25×1.25	11.38
	1.5×1.5	11.26
2.25	0.5×0.5	12.24
	0.75×0.75	12.32
	1×1	12.28
	1.25×1.25	11.50
	1.5×1.5	11.30
2.5	0.5×0.5	12.20
	0.75×0.75	12.28
	1×1	12.38
	1.25×1.25	11.82
	1.5×1.5	11.48
2.75	0.5×0.5	12.16
	0.75×0.75	12.24
	1×1	12.32
	1.25×1.25	12.42
	1.5×1.5	11.90
3	0.5×0.5	12.14
	0.75×0.75	12.20
	1×1	12.28
	1.25×1.25	12.38
	1.5×1.5	12.50

Table 5: Influence of the distance d_{obs} between the obstacle and the exit and of the dimensions L_{obs} and l_{obs} on the evacuation time in the presence of an obstacle.

275 According to the results in Table 5, with an accurate choice of obstacle parameters (dimensions, position) the time of the pedestrian evacuation could be improved by putting an obstacle in the room.

The square-shaped obstacle that allows to get a smaller evacuation time is that with dimensions $1.5m \times 1.5m$ and located at $1m$ from the exit.

Our study confirms that a strategically placed obstacle near an exit can speed evacuations. Several simulations
280 varying its size, shape and orientation have to be performed and tailored to the space and to the width of the exit itself. The proposed technique is interesting for engineers and designers to improve and secure the evacuation of rooms as it executes faster than discrete deterministic model using a random change of some of its parameters.

5. Conclusions

This paper presents the development of a new approach to model crowd dynamics based on the kinetic theory
285 of active particles. The existence and uniqueness of the solution of the proposed mathematical model have been proven for large times thanks to the Banach fixed-point theorem, assuming that the internal interactions between

pedestrians are negligible. Numerical simulations using a scheme based on a splitting method have been performed. The proposed model is able to describe some characteristics of the dynamics of a crowd in a bounded domain (with walls, an exit and an obstacle) namely, avoidance and evacuation. Indeed, several cases were studied to show the ability of this model to reproduce pedestrian behavior, and the results were compared to those obtained with a deterministic approach. Finally, the influence of a square-shaped obstacle on the evacuation time is studied. Indeed, with a suitable choice of obstacle parameters (dimensions and position), it has been shown that the time of the pedestrian evacuation may become much shorter than without any obstacle.

Acknowledgments

The authors are grateful to the reviewers for their insightful remarks and corrections. Their feedback has greatly influenced the quality of this paper.

The authors would also like to thank Nicholas Collins-Craft for his help editing the English of this paper.

Appendix A:

Proof of Lemma

1. It is assumed that:

$$|\rho_1(t, x) - \rho_2(t, x)| \leq \exp(-\lambda t) \dots \times \left(\sum_{h=1}^n \sum_{k=1}^n |\psi_h^1(t, x - v \cos(\theta_h)t, y - v \sin(\theta_h)t) - \psi_k^2(t, x - v \cos(\theta_k)t, y - v \sin(\theta_k)t)| \right),$$

from the equation (27) and the hypothesis (A.1), (A.2.), let us note $B_{hk}(i)[\rho(t, \mathbf{x})] \leq 1$, the following estimates are then deduced:

$$\|\widehat{\Psi}[\psi^1, \psi^1](t) - \widehat{\Psi}[\psi^2, \psi^2](t)\|_1 \leq (c_\eta + nR(c_\eta L_B + L_\eta)) (\|\psi^1(t)\|_1 + \|\psi^2(t)\|_1) \|\psi^1(t) - \psi^2(t)\|_1, \quad (.1)$$

$$\|\widehat{\Upsilon}[\psi^1]\widehat{\psi}^1(t) - \widehat{\Upsilon}[\psi^2]\widehat{\psi}^2(t)\|_1 \leq (c_\eta + L_\eta R) (\|\psi^1(t)\|_1 + \|\psi^2(t)\|_1) \|\psi^1(t) - \psi^2(t)\|_1, \quad (.2)$$

$$\|\widehat{\Lambda}[\psi^1](t) - \widehat{\Lambda}[\psi^2](t)\|_1 \leq (c_\mu + nRL_\mu) \|\psi^1(t) - \psi^2(t)\|_1. \quad (.3)$$

According to estimates (.1)-(.3), the estimate (28) is obtained with

$$C_1 = 2c_\eta + R(nc_\eta L_B + (n+1)L_\eta),$$

$$C_2 = 2c_\mu + (n+1)RL_\mu.$$

2. Since $\widehat{\Psi}_i[\psi, \psi](t, \mathbf{x}) \geq 0$ and $\widehat{\Lambda}_i[\psi](t, \mathbf{x}) \geq 0$ because $\psi_i(\mathbf{x}) \geq 0$, then $(\widehat{A}\psi)_i(t, \mathbf{x}) \geq 0$ if $\lambda - \mu[\rho] - \widehat{\Upsilon}_i[\psi](t, \mathbf{x})\exp(-\lambda t) \geq 0$,

from (A.1) and the equation (27), it is deduced that:

$$\Upsilon_i[\psi](t, \mathbf{x}) \leq R\exp(\lambda t)c_\eta|V|, \quad i = 1 \dots n,$$

so for that $\widehat{A}(\psi)_i(t, \mathbf{x}) \geq 0$, it is enough to choose $\lambda \geq \lambda_0 = Rc_\eta|V| + c_\mu$.

3. Let us note that if $P_h(i) \leq 1$, from (A.1) and equation (27), it can be deduced that, for $i = 1, \dots, n$,

$$\begin{aligned}\widehat{\Psi}_i[\boldsymbol{\psi}, \boldsymbol{\psi}](t, \mathbf{x}) &\leq c_\eta |V| R^2 \exp(2\lambda t), \\ \widehat{\Lambda}_i[\boldsymbol{\psi}](t, \mathbf{x}) &\leq c_\mu \exp(\lambda t),\end{aligned}$$

hence for a choice of R such that:

$$R \geq \sum_{i=1}^n \|\phi_i\|_\infty = R_1,$$

and a time: t such that

$$t \leq T = \frac{1}{\lambda} \ln \left(1 + \frac{\lambda}{nR(c_\eta R|V| + c_\mu)} \left(R - \sum_{i=1}^n \|\phi_i\|_\infty \right) \right) := T_0, \quad (4)$$

we obtain the relation (31).

4. Let $\boldsymbol{\psi} \in \mathbb{X}_T$, $T \geq 0$, according to the equation (9), (6) for $P_h(i)$, $B_{hk}(i)$, the hypothesis (A.1.), and using the following variable changes:

$$\begin{aligned}(z_1, z_2) &\leftarrow (x + v(\cos(\theta_i) - \cos(\theta_h))t, y + v(\sin(\theta_i) - \sin(\theta_h))t), \\ (w_1, w_2) &\leftarrow (x - v \cos(\theta_i)t, y - v \sin(\theta_i)t).\end{aligned}$$

We show that:

$$\|\widehat{\Psi}[\boldsymbol{\psi}, \boldsymbol{\psi}](t)\|_1 \leq c_\eta \|\boldsymbol{\psi}(t)\|_1^2, \quad (5)$$

$$\|\widehat{\Upsilon}[\boldsymbol{\psi}]\widehat{\boldsymbol{\psi}}(t)\|_1 \leq c_\eta \|\boldsymbol{\psi}(t)\|_1^2, \quad (6)$$

$$\|\widehat{\Lambda}[\boldsymbol{\psi}](t)\|_1 \leq c_\mu \|\boldsymbol{\psi}(t)\|_1. \quad (7)$$

From the relations (.5) - (.7) it can be found:

$$\|\mathbf{A}\boldsymbol{\psi}(t)\|_1 \leq \|\boldsymbol{\phi}\|_1 + \frac{2}{\lambda} c_\eta (1 - \exp(-\lambda t)) \|\boldsymbol{\psi}\|_{\mathbb{X}_T}^2 + (\lambda + 2c_\mu) t \|\boldsymbol{\psi}\|_{\mathbb{X}_T}, \quad (8)$$

since $2c_\mu \leq C_1$ and $2c_\eta \leq C_2$, hence the estimate (34) becomes:

$$\|\mathbf{A}\boldsymbol{\psi}\|_{\mathbb{X}_T} \leq \|\boldsymbol{\phi}\|_1 + \frac{C_1}{\lambda} \|\boldsymbol{\psi}\|_{\mathbb{X}_T}^2 + (\lambda + C_2) T \|\boldsymbol{\psi}\|_{\mathbb{X}_T}. \quad (9)$$

This ends the proof of the Lemma.

Appendix B:

The following equation

$$(E) : \|\boldsymbol{\phi}\|_1 + \frac{1}{\lambda} C_1 a_0^2 \|\boldsymbol{\phi}\|_1^2 + (C_2 + \lambda) T a_0 \|\boldsymbol{\phi}\|_1 = a_0 \|\boldsymbol{\phi}\|_1$$

has a solution a_0 if,

$$\|\boldsymbol{\phi}\|_1 \leq \min \left\{ \frac{(n-1)^2 c_\mu}{8n^2 c_\eta}, \frac{(n-1)^2 c_\eta |V|}{(4n^2 (nc_\eta L_B + (n+1)L_\eta))} \right\}.$$

Indeed, the discriminant of the equation (E) is given by,

$$\Delta_0 = ((C_2 + \lambda) T - 1)^2 - 4 \frac{C_1}{\lambda} \|\boldsymbol{\phi}\|_1.$$

$\Delta_0 \geq 0$ if $((C_2 + \lambda)T - 1)^2 \geq 4\frac{C_1}{\lambda}\|\phi\|_1$.

310 According to equation (35) and for $R \geq R_1$, $\lambda = \lambda_0 = c_\eta R|V| + c_\mu$,

$$T = \frac{1}{\lambda + C_2} \ln \left(1 + \frac{\lambda}{nR(c_\eta R|V| + c_\mu)} \left(R - \sum_{i=1}^n \|\phi_i\|_\infty \right) \right),$$

by using the following inequality $\ln(1+x) \leq x$, for $x \geq 0$

$$(\lambda + C_2)T \leq \frac{1}{n},$$

which implies,

$$(\lambda + C_2)T - 1 \leq \frac{1-n}{n},$$

then,

$$[(\lambda + C_2)T - 1]^2 \geq \frac{(1-n)^2}{n^2}.$$

Hence, if we have

$$4\frac{C_1}{\lambda}\|\phi\|_1 \leq \frac{(1-n)^2}{n^2}$$

then we get: $4\frac{C_1}{\lambda}\|\phi\|_1 \leq ((C_2 + \lambda)T - 1)^2$, by taking

$$\|\phi\|_1 \leq \frac{(1-n)^2}{n^2} \frac{\lambda}{4C_1},$$

hence,

$$\|\phi\|_1 \leq \frac{(1-n)^2}{4n^2} \frac{Rc_\eta|V| + c_\mu}{(2c_\eta + R(nc_\eta L_B + (n+1)L_\eta))} := \varphi^*(R).$$

Moreover,

$$\|\phi\|_1 \leq \underset{R \geq 0}{\operatorname{argmin}} \{\varphi^*(R)\}.$$

By studying the following function :

$$\varphi^* : R \rightarrow \varphi^*(R), \quad \text{with } R \in [0, +\infty[,$$

we have :

$$\underset{R \geq 0}{\operatorname{argmin}} \{\varphi^*(R)\} = \min \left\{ \frac{(n-1)^2 c_\mu}{8n^2 c_\eta}, \frac{(n-1)^2 c_\eta |V|}{(4n^2 (nc_\eta L_B + (n+1)L_\eta))} \right\}$$

in particular for $R > R_1$, we have:

$$\underset{R > R_1}{\operatorname{argmin}} \{\varphi^*(R)\} = \min \left\{ \frac{(n-1)^2 c_\mu}{8n^2 c_\eta}, \frac{(n-1)^2 c_\eta |V|}{(4n^2 (nc_\eta L_B + (n+1)L_\eta))} \right\} := \varphi^0.$$

References

- [1] M. Takashi, T. Akiyasu, I. Mayuko, S. Kohta and U. Daishin. *Effects of an obstacle position for pedestrian evacuation: SF model approach*. Springer International Publishing, Cham, 2015.
- [2] E. Cristiani, B. Piccoli and A. Tosin. *Multiscale modeling of pedestrian dynamics*. Springer International Publishing, Berlin, 2014.
- 315 [3] P. Argoul and B. Kabalan. *Pedestrian trajectories and collisions in crowd motion*. Springer Berlin Heidelberg, Berlin, Heidelberg, 2017.

- [4] D. Helbing and P. Molnár . Social force model for pedestrian dynamics. *Phys. Rev. E*, 51:4282–4286, May 1995.
- [5] D. Helbing, P. Molnár, I. J. Farkas and K. Bolay. Self-organizing pedestrian movement. *Environment and Planning B: Planning and Design*, 28:361–383, May 2001.
- 320 [6] R. L. Hughes. A continuum theory for the flow of pedestrians. *Transportation Research Part B: Methodological*, 36(6):507 – 535, 2002.
- [7] J. P. Agnelli, F. Colasuonno and D. Knopoff . A kinetic theory approach to the dynamics of crowd evacuation from bounded domains. *Mathematical Models and Methods in Applied Sciences*, 25(01):109–129, 2015.
- [8] N. Bellomo, A. Bellouquid and D. Knopoff. From the microscale to collective crowd dynamics. *Multiscale Modeling & Simulation*,
325 11(3):943–963, 2013.
- [9] N. Bellomo and A. Bellouquid. On the modeling of crowd dynamics: Looking at the beautiful shapes of swarms. *Networks and Heterogeneous Media*, 6(3):383–399, 2011.
- [10] N. Bellomo and L. Gibelli. Toward a mathematical theory of behavioral-social dynamics for pedestrian crowds. *Mathematical Models and Methods in Applied Sciences*, 25(13):2417–2437, 2015.
- 330 [11] N. Bellomo and A. Bellouquid. On multiscale models of pedestrian crowds from mesoscopic to macroscopic. *Commun. Math. Sci*, 13:1649–1664, 2015.
- [12] N. Bellomo. *Modeling complex living systems*. Birkhuser Basel, Birkhuser Boston, 2008.
- [13] V.V. Aristov. *Direct methods for solving the Boltzmann equation and study of nonequilibrium flows*. Springer Netherlands, Boston, 2001.
- 335 [14] P. Barbante, A. Frezzotti and L. Gibelli. A kinetic theory description of liquid menisci at the microscale. *Kinetic and Related Models*, 8(2):235–254, 2015.
- [15] N. Bellomo and A. Bellouquid. Global solution to the cauchy problem for discrete velocity models of vehicular traffic. *Journal of Differential Equations*, 252(2):1350 – 1368, 2012.
- [16] A. Bellouquid , E. D. Angelis and L. Fermo. Towards the modeling of vehicular traffic as a complex system: A kinetic theory
340 approach. *Mathematical Models and Methods in Applied Sciences*, 22(supp01):1140003, 2012.
- [17] N. Bellomo and L. Gibelli. Behavioral crowds: Modeling and Monte Carlo simulations toward validation. *Computers and Fluids*, 141:13 – 21, 2016. Advances in Fluid-Structure Interaction.
- [18] G. Marsan, Ajmone, N. Bellomo and L. Gibelli. Stochastic evolutionary differential games toward a systems theory of behavioral social dynamics. *Mathematical Models and Methods in Applied Sciences*, 26(06):1051–1093, 2016.
- 345 [19] G. K. Still. *Crowd dynamics*. PhD thesis, University of Warwick, 2000.
- [20] J. Geiser, G. Tanoğlu and N. Gücüyenlen . Higher order operator splitting methods via Zassenhaus product formula: Theory and applications. *Computers and Mathematics with Applications*, 62(4):1994 – 2015, 2011.
- [21] M.-Y Kim and E.-J Park. An upwind scheme for a nonlinear model in age-structured population dynamics. *Computers and Mathematics with Applications*, 30(8):5 – 17, 1995.
- 350 [22] J.C. Lopez-Marcos. An upwind scheme for a nonlinear hyperbolic integro-differential equation with integral boundary condition. *Computers and Mathematics with Applications*, 22(11):15 – 28, 1991.